REPURPOSING OF ANTIPSYCHOTIC AGENT TRIFLUOPERAZINE FOR MULTIPLE MYELOMA TREATMENT: IN VITRO STUDIES

A THESIS SUBMITTED TO
THE GRADUATE SCHOOL OF NATURAL AND APPLIED SCIENCES
OF
MIDDLE EAST TECHNICAL UNIVERSITY

BY

HEVAL ATAŞ

IN PARTIAL FULFILLMENT OF THE REQUIREMENTS
FOR
THE DEGREE OF MASTER OF SCIENCE
IN
BIOTECHNOLOGY

AUGUST 2016

Approval of the thesis:

REPURPOSING OF ANTIPSYCHOTIC AGENT TRIFLUOPERAZINE FOR MULTIPLE MYELOMA TREATMENT: IN VITRO STUDIES

submitted by **HEVAL ATAŞ** in partial fulfillment of the requirements for the degree of **Master of Science in Biotechnology Department, Middle East Technical University by**,

Prof. Dr. Gülbin Dural Ünver _____
Dean, Graduate School of Natural and Applied Sciences

Assoc. Prof. Dr. Çağdaş Devrim Son _____
Head of Department, Biotechnology

Assoc. Prof. Dr. Can Özen _____
Supervisor, Biotechnology Dept., METU

Dr. Aslı Erdoğ _____
Co-Supervisor, Düzce Teknopark A.Ş.

Examining Committee Members:

Asst. Prof. Dr. Yeşim Soyer _____
Food Engineering Dept., METU

Assoc. Prof. Dr. Can Özen _____
Biotechnology Dept., METU

Asst. Prof. Dr. Harun Koku _____
Chemical Engineering Dept., METU

Asst. Prof. Dr. Özgül Persil Çetinkol _____
Chemistry Dept., METU

Assoc. Prof. Dr. Ilgaz Akata _____
Biology Dept., Ankara University

Date: 19.08.2016

I hereby declare that all information in this document has been obtained and presented in accordance with academic rules and ethical conduct. I also declare that, as required by these rules and conduct, I have fully cited and referenced all material and results that are not original to this work.

Name, Last name: HEVAL ATAŞ

Signature:

ABSTRACT

REPURPOSING OF ANTIPSYCHOTIC AGENT TRIFLUOPERAZINE FOR MULTIPLE MYELOMA TREATMENT: IN VITRO STUDIES

Ataş, Heval
M.S., Department of Biotechnology
Supervisor: Assoc. Prof. Dr. Can Özen
Co – Supervisor: Dr. Aslı Erdoğ

August 2016, 55 pages

Multiple Myeloma (MM) is a hematological malignancy resulting from the proliferation of plasma B cells in the bone marrow. MM accounts for 20 % of deaths from blood cancers and 2 % of deaths from all cancers. Although there have been remarkable developments in the treatment of MM, it is still an incurable disease due to the drug resistance problem. Therefore, development of novel therapies is especially important for MM patients. Drug repurposing is one of the promising strategies to discover new anticancer agents. It considerably reduces the cost and time spent, and bypasses safety concerns necessary for de novo drug discovery.

Trifluoperazine (TFP) is an FDA-approved antipsychotic drug mainly used in the treatment of schizophrenia. Apart from its fundamental antipsychotic effects, there are several studies showing its anticancer potential in various cancer types such as leukemia, lung, melanoma, prostate, and breast. The aim of this study was to investigate the anticancer potential and mechanism of TFP on U266 MM cell line. Firstly, dose and time dependent inhibitory and cytotoxic effect of TFP was studied. Then, three different apoptosis studies were performed. It was followed by cell cycle

analysis to investigate its antiproliferative effect. Lastly, its combination potential with cisplatin was evaluated.

TFP showed dose and time-dependent inhibitory and cytotoxic effect on U266 cell line. Its IC_{50} value was determined as 15.4 ± 0.7 μM. Caspase-3 and AnnexinV-PE / 7-AAD assays indicated apoptosis while JC-1 gave negative results. Cell cycle analysis showed that TFP did not induce cell cycle arrest in U266 cell line. TFP-cisplatin combination was additive with higher doses of TFP, and slightly antagonistic with lower doses of TFP. Based on these preliminary findings, TFP warrants further in-depth mechanistic studies and *in vivo* experiments to evaluate its therapeutic potential for MM treatment.

Keywords: Multiple myeloma, drug repurposing, trifluoperazine, apoptosis

ÖZ

ANTİPSİKOTİK AJAN TRİFLUOPERAZİN' İN MULTİPL MİYELOM TEDAVİSİ İÇİN YENİDEN HEDEFLENDİRİLMESİ: İN VİTRO ÇALIŞMALAR

Ataş, Heval
Yüksek Lisans, Biyoteknoloji Bölümü
Tez Yöneticisi: Doç. Dr. Can Özen
Yardımcı Tez Yöneticisi: Dr. Aslı Erdoğ

Ağustos 2016, 55 sayfa

Multipl Myelom (MM), kemik iliğindeki plazma B hücrelerinin proliferasyonundan kaynaklı bir hematolojik malignensidir. Kan kanseri ölümlerinin % 20' sine ve tüm kanser ölümlerinin % 2' sine tekabül etmektedir. MM tedavisine dair çok önemli gelişmeler olsa da, ilaç direnci problemi dolayısıyla bu hastalığın hala kesin bir tedavisi yoktur. Dolayısıyla yeni terapilerin geliştirilmesi özellikle MM hastaları için çok önemlidir. İlaçların yeniden hedeflendirilmesi, yeni antikanser ajanlarının keşfinde umut vaad eden stratejilerden biridir. Bu yöntem, harcanan maliyeti ve zamanı önemli derecede azaltır ve yeni bir ilaç geliştirmek için gerekli olan bazı kontrol aşamalarından muaf tutulur.

Esas olarak şizofreni tedavisinde kullanılan trifluoperazin (TFP), FDA onaylı antipsikotik bir ilaçtır. Belli başlı antipsikotik etkilerinin dışında, TFP' nin lösemi, akciğer, melanom, prostat ve meme gibi çeşitli kanser tipleri üzerindeki antikanser potansiyelini gösteren birçok çalışma bulunmaktadır. Bu çalışma, TFP' nin U266 MM hücre hattı üzerindeki antikanser potansiyelinin ve mekanizmasının araştırılmasını amaçlamaktadır. Bu amaç doğrultusunda ilk olarak, TFP' nin doza ve

zamana bağlı inhibe edici ve sitotoksik etkisi çalışılmıştır. Daha sonra, üç farklı apoptoz çalışması yürütülmüştür. Onu takiben, antiproliferatif etkisini araştırmak için hücre döngüsü analizi yapılmıştır. Son olarak, sisplatin ile kombinasyon potansiyeli değerlendirilmiştir.

TFP, U266 MM hücre hattı üzerinde doza ve zamana bağlı inhibe edici ve sitotoksik etki göstermiştir. IC_{50} değeri 15.4 ± 0.7 μM olarak belirlenmiştir. Apoptoz çalışmalarında, JC-1 negatif sonuçlar verirken, AnnexinV-PE / 7-AAD assaylerinde apoptozun indüklendiği gösterilmiştir. Hücre döngüsü analizi sonuçları, TFP' nin U266 hücre hattı üzerinde hücre döngüsünü durdurucu etkisinin olmadığını göstermiştir. TFP-sisplatin kombinasyonu TFP nin yüksek dozlarında additif etki gösterirken, düşük dozlarında kısmen antagonistik etki göstermiştir. Bu ön bulgulara dayanarak, TFP' nin MM tedavisindeki terapötik potansiyeli daha derin mekanistik çalışmalarla ve *in vivo* deneylerle araştırılabilir.

Anahtar kelimeler: Multipl myelom, ilaç yeniden hedeflendirme, trifluoperazin, apoptoz

To my little smurfs Öykü and Kuzey,

ACKNOWLEDGEMENTS

First of all, I would like to express my deepest gratitude to my supervisor Assoc. Prof. Dr. Can Özen for not only his academic support, patience, and encouragement, but also for his valuable advices in every aspect. I am also grateful to my co-supervisor Dr. Aslı Erdoğ for her valuable support and guidance.

I would like to acknowledge Prof. Dr. Mayda Gürsel for her suggestions and to thank her lab members for their help. I would like to thank my thesis committee members Asst. Prof. Dr. Yeşim Soyer, Asst. Prof. Dr. Harun Koku, Asst. Prof. Dr. Özgül Persil Çetinkol, and Assoc. Prof. Dr. Ilgaz Akata for their valuable criticism and advices. I am also grateful to Asst. Prof. Dr. Erhan Astarcı for his contributions.

I would also like to thank my graduated lab mates İpek Durusu, Ayşenur Biber, Efe Erdeş, and Tuğba Somay Doğan for their friendships and contributions. I am especially so thankful to my lab colleagues Hazal Hüsnügil, Selin Gerekçi, and Ezgi Güleç for their significant contributions and help for experiments. Most importantly, their makatable friendships and invaluable support motivated me to finish this study. I should also express my gratitude to Taylan Güvenilir for his endless encouragement and emotional support.

Many thanks to TÜBİTAK for the financial support by BİDEB 2210 Domestic M.Sc. scholarship.

Lastly, I would like to express my sincere gratitude to my family. Especially, I have to thank my mother Aysel Ataş and my father Halil Ataş for their unconditional support. They could not help me academically, but they taught me to struggle and never lose the hope, which is the most precious treasure for me.

TABLE OF CONTENTS

LIST OF TABLES

TABLES

LIST OF FIGURES

FIGURES

LIST OF ABBREVIATIONS

ABC: ATP Binding Cassette

ANOVA: Analysis of Variance

ATP: Adenosine Triphosphate

BID: Bis in Die (twice a day)

BLM: Belomycin

BPD: Bepridil

CaM: Calmodulin

CDK: Cyclin-dependent Kinase

CI: Combination Index

Cis: Cisplatin

CPZ: Chlorpromazine

CSC: Cancer Stem Cell

DISC: Death Inducing Signaling Complex

DMSO: Dimethyl Sulfoxide

DNA: Deoxyribonucleic Acid

DOX: Doxorubicin

FDA: Food and Drug Administration

FGAs: First Generation Antipsychotics

HLP: Haloperidol

HT: Hyperthermia

IL-6: Interleukin-6

IC_{50}: Half maximal inhibitory concentration

IMiDs: Immunomodulatory Drugs

MDR: Multidrug Resistance

MM: Multiple Myeloma

MMP: Mitochondrial Membrane Permeabilization

MP: Melphalan plus Prednisone

MPT: Mitochondrial Permeability Transition

MRP: MDR Related Protein

NSCLC: Non-Small Cell Lung Cancer

PBS: Phosphate-Buffered Saline

PGP: P-glycoprotein

Phts: Phenothiazines

PI: Propidium Iodide

PI: Proteasome Inhibitor

PS: Phosphatidylserine

RFU: Relative Fluorescence Unit

RNase: Ribonuclease

SD: Standard Deviation

SEM: Standard Error of the Mean

TdT: Dideoxynucleotidyl

TFP: Trifluoperazine

TMX: Tamoxifen

TNBC: Triple Negative Breast Cancer

TNF: Tumor Necrosis Factor

CHAPTER 1

INTRODUCTION

1.1 Multiple Myeloma

1.1.1 Definition

Multiple Myeloma (MM) is a hematological malignancy resulting from the proliferation of plasma B cells in the bone marrow, which is driven by various factors containing tumor necrosis factor (TNF) alpha and interleukin 6 (IL-6) [1]. Healthy plasma cells produce antibodies against antigens that play an essential role in the immune system. However, malignant plasma cells produce abnormal antibodies called M proteins, which accumulate in large quantities and cause osteolytic lesions in the bone (Figure 1). Common symptoms of MM are bone pain and fractures, anemia, frequent infections, and renal failure [2].

1.1.2 Epidemiology

MM is the second most common hematological malignancy that accounts for 20 % of deaths from blood cancers and 2 % of deaths from all cancers. The majority of people diagnosed with MM are 65 years or older. Survival range of MM patients is around 1-10 years and 5-year survival rate is 48.5 % [1,3]. It is two times more common in black people than white people and slightly more common in males compared to females [4].

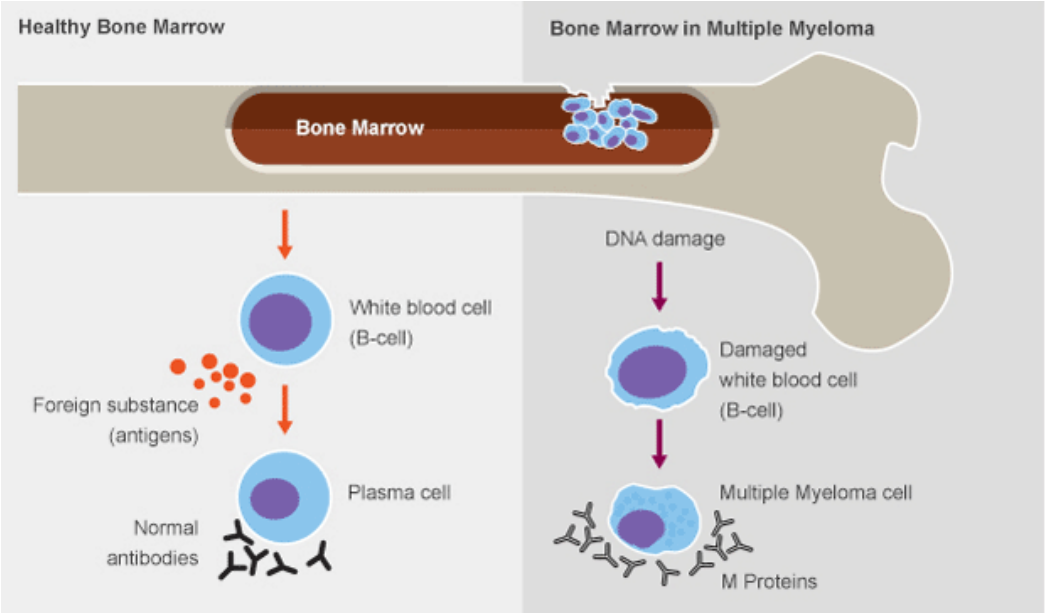

Figure 1. Normal plasma cell vs. MM cell in the bone marrow [5]

1.1.3 History of Multiple Myeloma Treatment

The first well-documented case of MM belonging to Sarah Newbury, a 39 year old woman, was reported by Samuel Solly in 1844. He tried to treat the disease with the rhubarb pill and infusion of orange peel. 4 years after symptoms arise, when finding a red substance in the place of the bone marrow at autopsy, Solly thought the disease was an inflammation.

The case of Thomas Alexander McBean (49 years old) was the best known MM case. His urine was examined by Dr. Henry Bence Jones, who was a chemical pathologist, and an abnormal urine protein was identified as ‘hydrated deutoxide of albumen’ [4], which was later named Bence Jones protein, a urinary immunoglobulin free light chain still used in diagnosis of MM [6]. In 1845, his physician Thomas Watson prescribed steel and quinine, which resulted in rapid symptomatic improvement. However, his pain relapsed and he died in 1846 despite the use of different treatment methods.

In 1947, N. Alwall used urethane in MM therapy that achieved to increase hemoglobin levels, and to decrease bone marrow plasma cells in a patient. Urethane became the standard therapy of MM for over 15 years. However, further studies showed that there was no difference between the effects of urethane and a cherry & cola flavored syrup placebo.

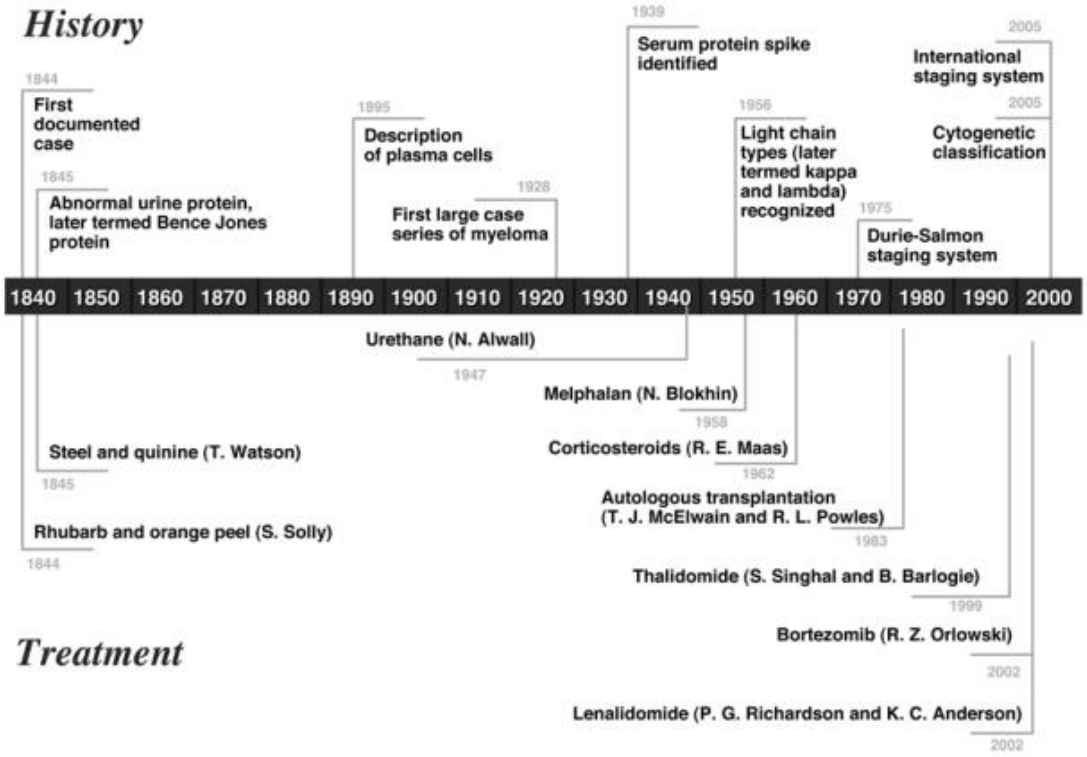

Figure 2. Timeline representing the history and treatment of MM from 1840s to the present [4]

In 1958, Blokhin et al. reported the success of melphalan, an alkylating nitrogen mustard, in the treatment of MM.

In 1962, corticosteroids were first tested by R. Maas, who used prednisone in a placebo controlled trial for MM treatment.

In 1970s, melphalan plus prednisone (MP) was used in combined with therapeutic agents such as carmustine, cyclophosphamide, and vincristine. MP combination was used as the main strategy in MM treatment for decades.

Autologous bone marrow transplantation was first reported by McElwain and Powles in 1983 (Figure 2) [4].

1.1.4 Current Therapy

Since the end of the 20th century, there has been remarkable findings and developments in the pathogenesis and treatment of MM. Genetic alterations in malignant plasma cells and interactions between these cells and the bone marrow microenvironment have provided new aspects to MM therapy [7].

Thalidomide, an immunomodulatory drug, has become a significant treating agent for MM after its high cytotoxic potency on malignant plasma cells was discovered. Although its antiangiogenic effects revealed its potential in MM treatment initially, its modulatory effects on cell signaling pathways associated with cancer have been demonstrated later (e.g. the inhibition of NF-kB activation), and linked closely to the proliferation, invasion, and metastasis of tumors [8].

It was followed by the development of a first-generation proteasome inhibitor (PI) bortezomib, which not only targets MM cell but also targets its interaction with the bone marrow microenvironment. In MM cells, bortezomib activates c-Jun NH2 terminal kinase by inducing cell stress response and triggers cell cycle arrest, followed by caspase-dependent apoptosis [9].

Then, new immunomodulatory drugs (IMiDs) as thalidomide derivatives, lenalidomide and pomalidomide, were developed. Recently, carfilzomib and ixazomib, which are second generation PIs, have been approved by the FDA. Furthermore, the deacetylase inhibitor panobinostat and monoclonal antibodies

elotuzumab, nivolumab/pembrolizumab, and isatuximab/daratumumab targeting SLAMF7, PD-1 and CD38 proteins, respectively, have emerged as a targeted therapy for MM [7]. Although there is still no way to cure MM completely, these improvements increase the life quality of patients, extending their survival to 10 years [1].

1.1.5 Drug Resistance and Combination Therapy

The main factor in the failure of chemotherapy is the resistance developed by cancer cells against therapeutic agents. This resistance mechanism involves the reduction or retention in drug accumulation, overproduction of the target enzyme or changes in its conformation, reduced activation or increased catabolism of drug [10].

P-glycoprotein (PGP) and multidrug resistance (MDR) - related protein (MRP) are two drug efflux pumps belonging to the ATP binding cassette (ABC) superfamily of membrane proteins that actively pump out drugs from the cell membrane [10]. In resistant cancer cells, these proteins are overexpressed and protect the cells from the toxic effects of drugs. They are one of the main targets in cancer treatment due to their significant role in malignant cells [11].

More specifically, in MM, neoplastic plasma cells interact with the bone marrow microenvironment including bone marrow stromal cells, osteoblasts, endothelial cells, and extracellular matrix. This interaction promotes the proliferation, migration, and drug resistance of these cells [12]. Furthermore, mutations in TP53, ACTG1, RB1, PRDM1, CYLD, TRAF3, BRAF, FAM46C, DIS3, NRAS, and KRAS genes with frequent intraclonal heterogeneity play essential role in drug resistance of MM cells [13].

To break drug resistance of cancer cells, one of the most commonly used therapeutic approaches is the combination of anticancer drugs in chemotherapy [14]. The main goal of combination therapy is to increase clinical efficacy with an acceptable dose

of toxicity that is tolerable by healthy cells. It is possible to overcome drug resistance by combining chemotherapeutic agents with the rationale that each of them targets different biochemical mechanisms in malignant cells, which allows for synergism to occur between targeted agents [15]. Based on this approach, the best strategy in combination therapy is to combine cytotoxic drugs with cytostatic drugs, chemosensitizers, antimetastatic drugs or biotherapies such as monoclonal antibodies or vaccines [14].

1.1.6 U266 Cell Line and The Role of p53

The U266 cell line was established from the blood of a 53 year old man in 1968, who had IgE secreting myeloma in terminal phase. The main characteristic of this cell line is having a single mutant p53 allele and overexpression of IL-6 [16]. Stable expression of wild-type p53 in U266 cells resulted in suppression of IL-6 gene expression, and caused to arrest on cell cycle [17]. U266 cell line is also resistant to Fas-mediated apoptosis and expresses high levels of Bcl-xL, an anti-apoptotic protein. Studies showed that blocking IL-6 receptor signaling by using JAK family kinases and Stat3 protein inhibited Bcl-xL expression and induced apoptosis [18].

p53 is a tumor suppressor protein that is involved in many critical cellular processes including transcription, genomic stability, DNA repair, cell cycle and apoptosis [19]. It restricts tumor growth by responding to cellular signals under stress conditions such as DNA damage, oncogene expression, nutrient depletion, and by limiting the cell proliferation under these conditions (Figure 3) [20]. Hence, it is one of the most comprehensively studied proteins in cancer research due to this critical role in the cell. When its role completely revealed in molecular level, it may help to identify significant molecular targets for treatment of cancer [21].

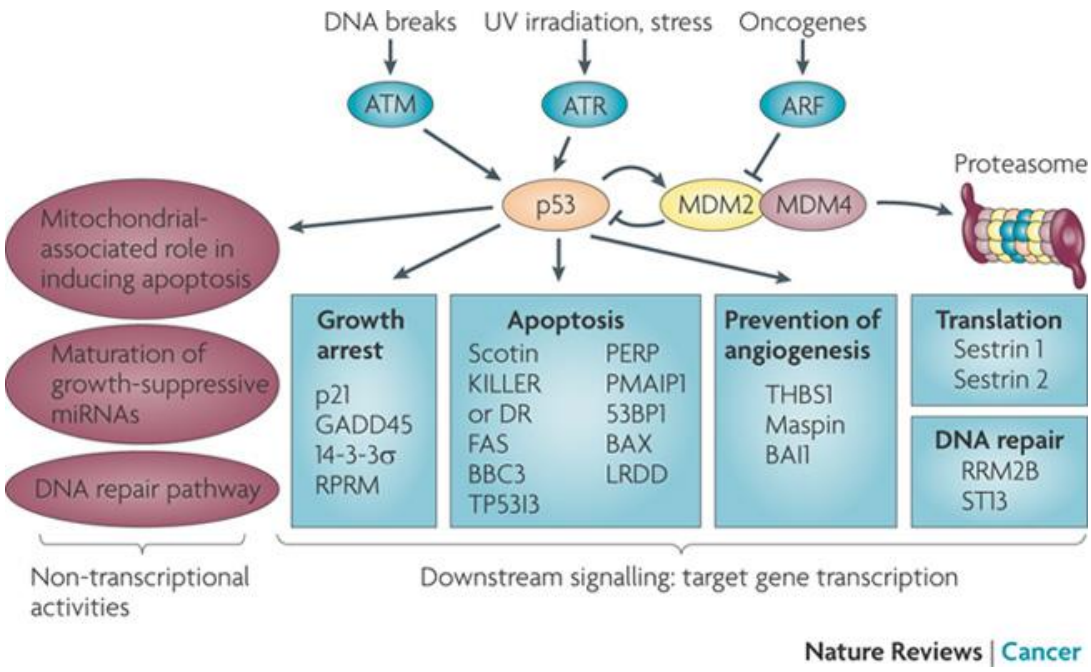

Figure 3. The p53 pathway [22]

1.2 Drug Repurposing for Cancer Therapy

Drug repurposing, also called drug repositioning or drug reprofiling, is the use of an existing drug for a novel therapeutic indication, which is based on the fact that different diseases share common molecular targets and pathways in the cell. It is one of the favourite approaches for pharmaceutical industry since it considerably reduces the cost and time, and bypasses safety concerns necessary to develop a novel drug. De novo drug discovery process requires 13 years on average and costs around $ 2 billion until to releasing on the market. In addition to design and production, it needs a lot of tests for toxicity, efficacy, pharmacokinetic and pharmacodynamic profiles. Unfortunately, most drugs fail to receive FDA approval even if they pass Phase I trials. Perhaps, the biggest advantage of drug repurposing is being already approved by FDA [8].

Table 1. Original and new anticancer indications of repurposed drugs [8].

Drug	Original Indication	New anticancer indication
Thalidomide	Antiemetic for pregnancy	Multiple myeloma
Aspirin	Analgesic, antipyretic	Colorectal cancer
Valproic acid	Antiepileptic	Leukemia, solid tumors
Celecoxib	Osteoarthritis, rheumatoid arthritis	Colorectal cancer, lung cancer
Statins	Myocardial infarction	Prostate cancer, leukemia
Metformin	Diabetes mellitus	Breast, adenocarcinoma, prostate, colorectal cancer
Rapamycin	Immunosuppressant	Colorectal cancer, lymphoma, leukemia
Methotrexate	Acute leukemia	Osteosarcoma, breast cancer, Hodgkin lymphoma
Zoledronic acid	Anti-bone resorption	Multiple myeloma, prostate cancer, breast cancer
Leflunomide	Rheumatoid arthritis	Prostate cancer
Wortmannin	Antifungal	Leukemia
Minocycline	Acne	Ovarian cancer, glioma
Vesnarinone	Cardioprotective	Oral cancer, leukemia, lymphoma
Thiocolchicoside	Muscle relaxant	Leukemia, multiple myeloma
Nitroxoline	Antibiotic	Bladder, breast cancer
Noscapine	Antitussive, antimalarial, analgesic	Multiple cancer types

This strategy is especially used in cancer drug development due to the opportunity to directly enter into the process of clinical trials. One of the best known examples of drug repurposing in cancer treatment is thalidomide. It was initially prescribed as a sedative, and mainly used as an antiemetic to prevent morning sickness in pregnant women. However, due to the occurrence of severe birth defects, it was withdrawn from the market in 1961. It is now one of the main chemotherapeutic drugs used in MM treatment. Table 1 shows a list of other repurposed anticancer drugs [8].

In this study, we investigated the anticancer effect of trifluoperazine, an FDA-approved antipsychotic drug mainly used in the treatment of schizophrenia, on MM cell line U266. There are three main criteria in choosing a drug for repurposing strategy: its price, availability in pure form, and novelty. Trifluoperazine is a cheap drug available as pure compound in many firms. Moreover, there is no in-depth mechanistic study of trifluoperazine on MM. In addition, being a phenothiazine derivative with piperazine side chain and trifluoromethyl substituent makes it a potent drug, structurally.

In our research group, there have been also other studies based on drug repurposing strategy. It has been shown that clofazimine, a riminophenazine compound mainly used in the treatment of leprosy, induced apoptosis and inhibited cell proliferation in U266 cell line [23]. Similarly, tricyclic antidepressant nortriptyline also showed an antiproliferative and apoptotic effect on U266 [24].

1.3 First Generation Antipsychotics

First generation antipsychotics (FGAs), also known as ‘typical antipsychotics’, were developed in the 1950s, and widely used for the treatment of various psychiatric disorders including schizophrenia, schizoaffective disorder, some forms of bipolar disorder and delusional disorders [25].

FGAs have been classified according to their chemical structure, which mainly includes phenothiazines (e.g. chlorpromazine, thioridazine, trifluoperazine), butyrophenones (e.g. haloperidol, droperidol) and thioxanthenes (e.g. flupentixol, thiothixene). Their common mode of action is the blockade of D2 family of dopamine receptors (Figure 4). Therapeutic activity of FGAs is presumably related to this blockade on mesolimbic pathway [26]. The blockade of dopamine D2 receptors by FGAs also affects mesocortical, nigrostriatal, and tuberoinfundibular pathways. For this reason, they induce secondary negative symptoms and cognitive impairments, extrapyramidal symptoms, and hyperprolactinemia as a result of overdose usage [27]. Moreover, they show additional side effects such as sedation, constipation and cardiovascular problems due to their other pharmacological activities [26].

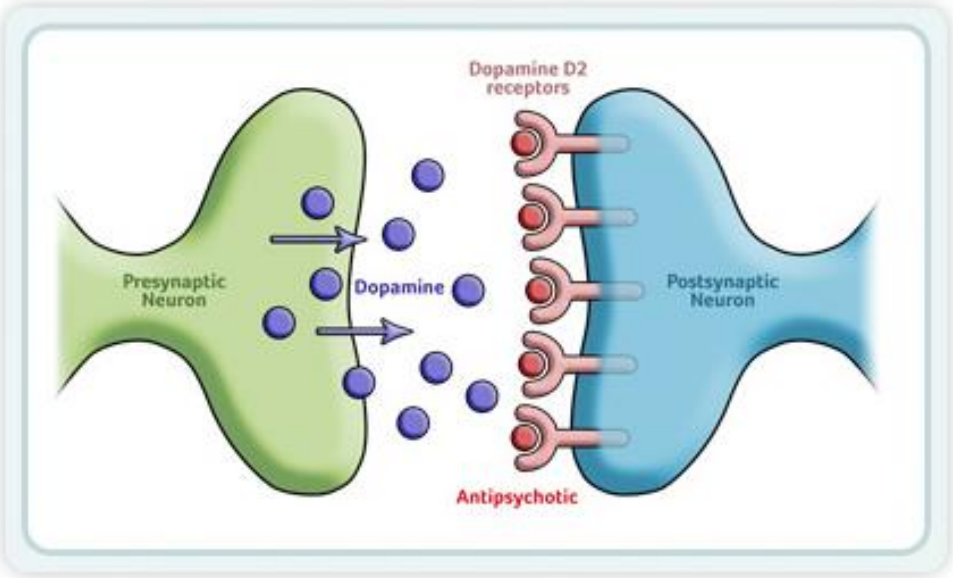

Figure 4. Blockade of dopamine D2 receptors by antipsychotics [28]

Phenothiazines are the first developed group of FGAs, and still widely used today. They are tricyclic compounds which contain two aromatic rings linked to the middle ring including nitrogen and sulfur atoms. There are three subclasses of phenothiazines based on differences in the composition of the side chain linked to the

nitrogen atom at position 10: aliphatics, piperidines, and piperazines, members of which differ in terms of potency and side effect profile (Figure 5). Another factor determining the efficacy of them is the presence of a substituent at the 2-position of the phenothiazine ring. Chlorpromazine, thioridazine, fluphenazine, perphenazine, and trifluoperazine are a few of the most known phenothiazines [29].

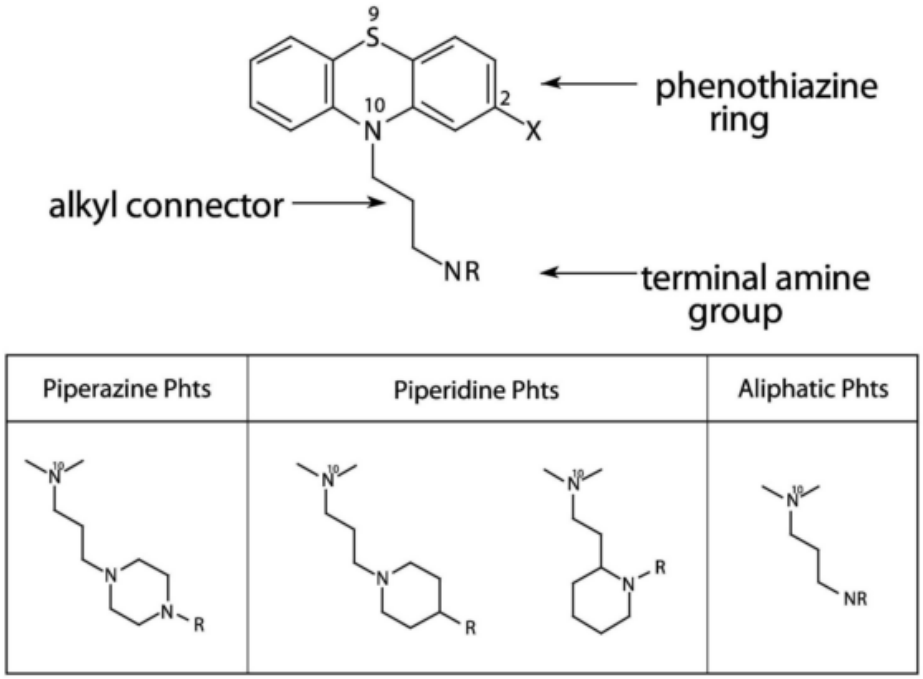

Figure 5. General chemical structure of phenothiazines (Phts) [30]

Apart from their fundamental antipsychotic effects, phenothiazines also exhibit diverse biological activities which are related with their potential anticancer effects including reversion of MDR due to downregulation of PGP, and inhibition of calmodulin, protein kinase C, and cell proliferation [30]. In addition to studies on anticancer potential of phenothiazines, it has been shown that patients with schizophrenia have lower risk to develop cancer than the general population. Moreover, these antipsychotic drugs can decrease symptoms related to the psychological state of cancer patients such as anxiety and insomnia [31].

1.3.1 Trifluoperazine

Trifluoperazine (TFP) is an FDA-approved first generation antipsychotic drug mainly used in the treatment of schizophrenia. As a member of FGAs, its antipsychotic activity is achieved by blockade of dopamine D2 receptor in the brain. Structurally, it is a phenothiazine derivative with piperazine side chain. However, its main efficacy appears to be related with the presence of trifluoromethyl substituent at the 2-position of the phenothiazine nucleus (Figure 6) [29,30].

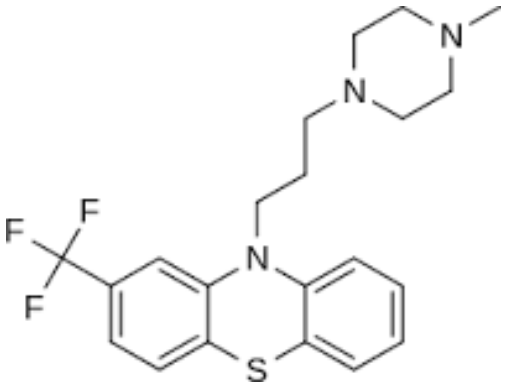

Figure 6. Chemical structure of trifluoperazine [32]

In addition to its dopamine D2 receptor blocking activity, TFP inhibits calmodulin (CaM) activity strongly. CaM is a multifunctional calcium binding protein expressed in all eukaryotic cells. It interacts with a diverse group of cellular proteins and takes part in signaling pathways, cell proliferation, regulation of cell motility and division. Therefore, CaM blocking activity of TFP could explain its antiproliferative and cytotoxic effect on many cancer cell lines [33].

By blocking CaM activity, it also causes to downregulation of PGP because PGP phosphorylation is regulated by CaM activated enzymes. Therefore, it inhibits multidrug resistance, and increases cellular chemosensitivity that makes it also a chemosensitizer candidate [30].

Table 2 shows additional targets of TFP identified in human.

Table 2. List of TFP targets identified in human [34]

Target	Action
D(2) dopamine receptor	antagonist
Neuron-specific vesicular protein calcyon	antagonist
Alpha-1A adrenergic receptor	antagonist
Calmodulin	inhibitor
Troponin C, slow skeletal and cardiac muscles	binding activity
Protein S100-A4	inhibitor
Xanthine dehydrogenase/oxidase	conversion inhibitor
UDP-glucuronosyltransferase 1-4	substrate
Cytochrome P450 1A2	substrate
Multidrug resistance protein 1	inhibitor

1.3.1.1 Previous Studies on Anticancer Effects of Trifluoperazine

There are various *in vitro* and *in vivo* studies showing anticancer effects of TFP in different cancer types such as leukemia, lymphoma, breast, lung, melanoma, prostate, and pancreatic cancer [35–41].

The anticancer effect of TFP was first described in 1982 by Tsuruo et. al. They showed the chemosensitizing activity of TFP on vincristine and Adriamycin (doxorubicin) resistant P388 leukemia cells. When cells were treated with TFP, intracellular levels of vincristine and Adriamycin increased. It resulted in the enhancement of the cytotoxicity of these agents, and circumvented the resistance of P388 cells against these drugs [42].

In 1983, Wei et. al. showed the growth inhibitory effect of TFP on MDA-MB-231 breast cancer cell line using a soft agar clonogenic assay. They determined the IC_{50} of TFP as 18 μM for continuous exposure, and 50 μM for 1 h exposure [43].

In 1986, Smith et. al. studied the effect of hyperthermia (HT, 44 ^{o}C) and TFP (30 μg/mL) on chromatin structure and belomycin (BLM)-induced DNA damage in EMT6 breast cancer cell line. They previously showed that when EMT6 cells treated with HT and TFP in a combined way, cytotoxic action of BLM on these cells increased. In this study, they showed that, there were significant changes in the DNA interaction with its protein matrix when cells treated with HT and TFP. Hence, they proposed that the cytotoxic enhancement on BLM-treated cells was related with the lethal DNA damage due to loss of DNA repair functions when cells treated with a combination of HT and TFP. This study indicated the potential of chromatin/DNA repair modifying approaches to overcome drug resistance in cancer cells, and provided a rational basis for the use of TFP in thermochemotherapy [44].

In 1988, Ganapathi et. al. showed the increase in the cytotoxic effect of doxorubicin (DOX) *in vivo* by treating male C57BL/6NCr mice injected with DOX-resistant sublines of B16-BL6 melanoma cells with a combination of DOX and 5 μM TFP. While the combination of DOX and TFP was significantly more effective than DOX alone, there was no correlation between the cellular DOX levels and magnitude of resistance after combination therapy. Hence, they inferred that DOX resistance modulatory effect of TFP was possibly due to mechanistic alterations in the cell instead of effects on drug accumulation or retention [45].

In 1989, a phase I trial of combined therapy with bleomycin and TFP was conducted by Hait et. al. There was no hematologic toxicity. The major toxicities were pulmonary and neurological. Two of nineteen patients showed partial responses and two had complete responses towards the therapy. Hait and his colleagues concluded that TFP could safely be given with bleomycin with a dose of < 9 mg BID [46].

In 1993, a phase II trial of DOX and TFP in metastatic breast cancer was conducted by Budd et. al. However, the combinatory effect of DOX and TFP did not show significant difference than the effect of DOX alone [47].

In 1996, Lehnert et. al. evaluated the effect of serum level on the ability of various chemosensitisers including TFP to reverse PGP-associated MDR. They tested these compounds on 8226/DOX6 and DOX40 myeloma cell lines in medium containing 10% fetal bovine serum and in 100% horse or human serum with drug sensitivity and accumulation assays. They treated cells with DOX alone and with combination of DOX and these chemosensitisers. Results showed that the MDR reversing activity of TFP and some other chemosensitizers was diminished by physiological serum protein concentrations [48].

In 1997, the induction of apoptosis in DOX-resistant P388/R84 murine leukemic cells was shown by Ramachandran et. al. Cells induced apoptosis only when treated with DOX and TFP in a combined way, not with DOX alone. The induction of apoptosis was achieved by terminal dideoxynucleotidyl (TdT) assay analyzed with flow cytometry, and confirmed with DNA fragmentation analysis [49].

In 1999, Pan et. al. demonstrated the induction of apoptosis in human cholangiocarcinoma cells treated with tamoxifen (TMX) and TFP separately. Human cholangiocarcinoma cells heterogeneously express Fas antigen on their surface. Based upon this fact, they isolated and cultured Fas-positive and Fas-negative surface expressing cells. When treating cells with TMX, TFP, and Fas antibody, only Fas-positive cells induced apoptosis. They suggested that this apoptotic cell death for both compound was probably mediated through the Fas/APO-1 signaling pathway via a CaM-dependent mechanism [50].

In 2004, Shin et. al. investigated the effect of Egr-1 expression on the TFP-induced growth inhibition in human U87MG glioma cells. Their findings suggested that TFP exhibits antiproliferative effect through up-regulation of Egr-1, which is a tumor

suppressor gene that has significant role in cell growth, differentiation and apoptosis [51].

In 2009, Chen et. al. investigated the anticancer effect of TFP in human A549 lung adenocarcinoma cell line. They demonstrated that TFP inhibited the cell growth in a dose- and time-dependent manner by inducing apoptosis. In addition to Annexin-V/PI results, the disruption of actin microfilaments, down-regulation of F-actin and anti-apoptotic Bcl-2 protein, up-regulation of pro-apoptotic Bax protein, and the increase in the phosphorylation levels of ERK and JNK proteins were indicating apoptosis [38].

In 2012, Yeh et. al. demonstrated the inhibition of cancer stem cell (CSC) tumor spheroid formation and down-regulation of the expression of CSC markers (CD44/CD133) in different non-small cell lung cancer (NSCLC) cell lines treated with TFP. In gefitinib-resistant lung cancer spheroids, TFP inhibited Wnt/b-catenin signaling pathway. Moreover, it showed synergistic effect when combined with gefitinib or cisplatin. Its inhibitory effect on the tumor growth was also shown in mouse models with lung cancer [52].

In 2014, Gross et. al. showed the antimetastatic effect of TFP on PC3 and C4-2b human prostate cancer cell lines. They demonstrated that TFP reduced the angiogenic and invasive potential of aggressive cancer cells by mediating b-catenin pathway likely through dopamine D2 receptor, which makes TFP a candidate for the treatment of prostate cancer as an antimetastasis agent [53].

In 2015, the enhancement of TRA-8-induced apoptosis on TRA-8-resistant pancreatic cancer cells treated with CaM antagonists TMX and TFP was shown by Yuan et. al. This enhancement was achieved by increasing death receptor 5 (DR5) expression and decreasing survival signals in DR5-associated DISC (death-inducing-signaling-complex). This study suggests the use of these CaM antagonists in a

combination with TRAIL-activating agents for the treatment of pancreatic cancer [33].

In 2016, FOXO-3 activation in bepridil (BPD)- and TFP-treated triple negative breast cancer (TNBC) cells was shown by Park et. al. both *in vitro* and *in vivo*. BPD and TFP inhibited Akt-pS473 phosphorylation and promoted FOXO3 nuclear localization. They decreased the expression of oncogenic c-Myc, KLF5, and dopamine D2 receptor, which are responsible for the increase in cancer stem cell-like populations in various tumors. Therefore, the decrease in the expression of these proteins suggests that BPD- and TFP-induced apoptosis might be related with a FOXO3-dependent mechanism in TNBC cells [37].

1.4 Aim of the Study

The aim of this study was to investigate the anticancer effect and mechanism of TFP on U266 MM cell line based on our preliminary findings from potency screening studies. This is the first in-depth cytotoxicity and apoptosis study of TFP on MM.

CHAPTER 2

MATERIALS AND METHODS

2.1 Chemicals

Drug formulations of atenolol (Nortan®), metoprolol (Beloc®), propranolol (Dideral®), chlorpromazine (Largactil®), trifluoperazine (Stilizan®), and haloperidol (Norodol®) were purchased from pharmacy. Pure forms of chlorpromazine, trifluoperazine and haloperidol were purchased from Alfa Aesar (Lancashire, United Kingdom). Cisplatin was purchased from Sigma-Aldrich (Taufkirchen, Germany). Chlorpromazine and trifluoperazine stocks were prepared in ultrapure water, haloperidol in DMSO as 10 mM stocks, and stored at -20 ^{o}C. Cisplatin was prepared in 0.9% NaCl as 1 mM stock, and. stored at room temperature.

2.2 Cell Culture

Human myeloma U266 cells were cultured in RPMI 1640 medium supplemented with 10% (v/v) fetal bovine serum, 1% (v/v) penicillin-streptomycin, 1% (v/v) non-essential aminoacids and 2.5 μg/mL plasmocin prophylactic as suspension culture, and incubated at 37 ^{o}C in 5% CO_2. For all assays, cell density was $1x10^5$ cells/mL at final volume. DMSO concentration in the culture medium for haloperidol treated cells and their controls fixed as 2% (v/v).

2.3 Cell Viability and Cytotoxicity Assays

Potency screening, dose response, time response, and combination assays were performed using CellTiter-Blue Cell Viability Assay (Promega / Madison, USA).

For all of these assays, 100 μL of untreated and treated cells with their blank control were seeded in 96-well plates ($1x10^4$ cells/well) with five technical replicates. After treatment, 20 μL of the assay reagent was added to each column and incubated for 4h at 37 ^oC in 5% CO_2 . Fluorescence signals were measured at 555 nm excitation and 595 nm emission using a SpectraMax Paradigm Multi-Mode Microplate Reader (Molecular Devices / Sunnyvale, USA). Data analysis was done by normalizing relative fluorescence unit (RFU) values of treated cells to untreated cells.

For potency screening, cell treatment with dissolved drug formulations of selected ß-blockers (atenolol, metoprolol, propranolol) and antipsychotics (chlorpromazine, trifluoperazine, haloperidol) was done at 100 μM (24h) for each compound. In the second screening assay, cells were treated with pure forms of chlorpromazine, trifluoperazine and haloperidol at 25 μM and 100 μM for 24 h.

For dose response, cells were treated with 12 doses of trifluoperazine (TFP), which are serially diluted from 10 mM TFP stock with sterilized ultrapure water, for 24 h. These doses were 0.5, 1, 2.5, 5, 7.5, 10, 12.5, 20, 25, 50, 75, and 100 μM, respectively. IC_{50} value of TFP was calculated on GraphPad (La Jolla, USA) Prism v5.0 using non-linear curve fitting, where x-axis is log values of these concentrations and y-axis is viability percentages at these concentrations.

For time response, cells were treated with 10 μM TFP for 12 h, 24 h, and 48 h. Normalization was done independently for each time point by normalizing RFU values of treated cells to untreated cells.

For combination assay, cells were treated with combined doses of TFP and cisplatin (Cis) for 24 h in 3 different sets of experiments. The first set of doses for TFP - Cis combination was 15 - 40, 15 - 20, 10 - 40, 10 - 20 μM, the second was 20 - 15, 15 - 15, 10 - 15 μM, and the last set was 25 - 10, 20 - 10, 15 - 10 μM, respectively. For each combined dose, Combination Index (CI) value was calculated using CompuSyn software (ComboSyn Inc. / Paramus, USA) according to growth inhibitory percentages of cells. Combined doses with CI values > 1.10 show antagonism, CI values between 0.90 - 1.10 show additivity, and CI values < 0.90 show synergism (Table 5 - App. B).

Cytotoxicity assay was performed using MultiTox-Fluor Multiplex Cytotoxicity Assay (Promega / Madison, USA), which measures cell viability and cytotoxicity simultaneously. 100 μL of untreated and treated cells with their blank control were seeded in 96-well plates ($1x10^4$ cells/well) with five technical replicates as in the cell viability assays mentioned above.

For this assay, cell treatment was done with 15 μM TFP for 24 h. After treatment, 100 μL of the assay reagent was added to each column and incubated for 3 h at 37 ^oC in 5% CO_2. Fluorescence signals were measured at 400 nm excitation and 505 nm emission for viability, and at 485 nm excitation and 525 nm emission for cytotoxicity using SpectraMax Paradigm Multi-Mode Microplate Reader (Molecular Devices / Sunnyvale, USA). Results were represented as RFU values without normalizing, which is not needed for this assay.

2.4 Cell Cycle Analysis

For cell cycle assay, cells were treated with 15 μM TFP for 24 h. Treated samples were fixed with 70% ethanol after a cold PBS wash and kept for 2 h on ice. Following centrifugation at 800 g for 5 min and PBS wash, 5 μL propidium iodide (25 μg/mL) and 90 μL RNase (3 mg/mL) was added. After completing the volume to 300 μL with PBS, cells were incubated at 37 ^oC for 30 min. Then, cell cycle analysis

was performed on Accuri C6 flow cytometer (BD Biosciences / San Diego, USA). To gate single cell population, FSC-A channel at x-axis and FSC-H channel at y-axis was chosen. 10,000 events were collected into the gate at medium speed of fluidics (35 μL/min). Fluorescence signals of gated samples stained with propidium iodide were measured on fluorescence intensity histogram, where x-axis represents FL2-A channel, and y-axis represents count. Borders of G0/G1, S, and G2/M phases were determined on the histogram, and their normalized values were plotted for untreated and treated cells.

2.5 Apoptosis Assays

Three apoptosis assays were conducted to evaluate mitochondrial membrane potential, caspase-3 activity, and cell membrane asymmetry of cells. MitoScreen Flow Cytometry Mitochondrial Membrane Potential Detection Kit, PE Active Caspase-3 Apoptosis Kit, and PE Annexin V Apoptosis Detection Kit I was supplied from BD Biosciences (San Diego, USA). Kit protocols were applied as recommended. Analysis of these assays was performed on Accuri C6 flow cytometer (BD Biosciences / San Diego, USA). Cells were gated, and 10,000 events were collected into the gate at medium speed of fluidics (35 μL/min).

For mitochondrial membrane potential assay, cell treatment was done with 15 μM TFP for 12, 24, and 48 h. Fluorescence signals of gated samples stained with JC-1 were measured on FL1-H channel at x-axis, and FL2-H channel at y-axis. Color compensation was set by subtracting 16.5 % of FL1 from FL2. Data analysis was done by normalizing gated depolarized and polarized state values for untreated and treated cells.

For caspase-3 activity assay, cells were treated with 15 μM TFP for 24 h. Fluorescence signals of gated samples incubated with PE conjugated anti-active caspase-3 antibody were measured on fluorescence intensity histogram, where x-axis

represents FL2-A channel, and y-axis represents count. An intensity threshold was drawn to determine caspase-3 activity percentage.

For cell membrane asymmetry assay, cell treatment was done with 15 μM TFP for 24 and 48 h. Fluorescence signals of gated samples stained with 7-AAD and PE conjugated Annexin V were measured on FL2-H channel at x-axis, and FL3-H channel at y-axis. Color compensation was set by subtracting 1.5 % of FL3 from FL2 and 21 % of FL2 from FL3. Cell population percentages of untreated and treated cells in live, early apoptosis, and late apoptosis stages were determined from quadrants on fluorescence intensity dot plots.

2.6 Statistical Analysis

For time response, mitochondrial membrane potential, cell membrane asymmetry, and cell cycle assays, statistical significance of results were determined using GraphPad Prism one-way ANOVA with Bonferroni correction for selected pairs. Statistical significance of cytotoxicity and caspase-3 activity assay results was determined using unpaired t-test with two-tails. Data were represented as Mean±SEM. Significance of differences was marked on the figures with asterisks. All statistical tests were conducted with 95% confidence interval.

CHAPTER 3

RESULTS

3.1 Potency Screening of Selected ß-blockers and Antipsychotics on Cell Growth Inhibition

As a preliminary study to investigate growth inhibitory effect of ß-blockers and antipsychotics on U266 (multiple myeloma cell line), drug formulations of selected ß-blockers (atenolol, metoprolol, propranolol) and antipsychotics (chlorpromazine, trifluoperazine, haloperidol) were screened by using CellTiter-Blue cell viability assay. This assay is based on the ability of live cells to metabolize resazurin into resorufin, which is highly fluorescent [54]. Cells were treated with 100 μM of each compound for 24 h. As shown in Figure 7, selected antipsychotics showed high decrease in cell viability, viability of which ranges between 1 - 15%, while ß-blockers did not affect viability considerably.

After this preliminary work, chlorpromazine (CPZ), trifluoperazine (TFP) and haloperidol (HLP) were tested in pure compound form. Treatment was done with two different doses (25 and 100 μM) of compounds. CPZ and TFP killed cells completely compared to HLP (26% viability) for 100 μM dose. For treatment with 25 μM dose, TFP (6% viability) was more effective than CPZ (39% viability) and HLP (89% viability) (Figure 8).

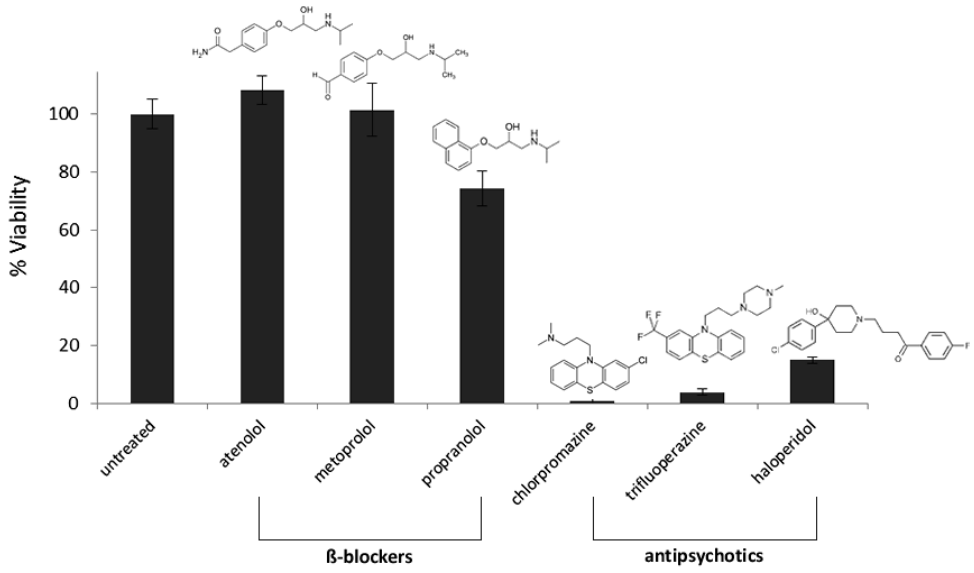

Figure 7. Effect of selected ß-blocker and antipsychotic formulations on viability of U266 cells at 100 µM (24 h) determined by CellTiter-Blue assay. Viability percentages are obtained by normalizing treated cells to untreated cells according to their RFU values. Compound structures are shown above the corresponding bars. Each column represents the Mean±SD of technical replicates (n=5).

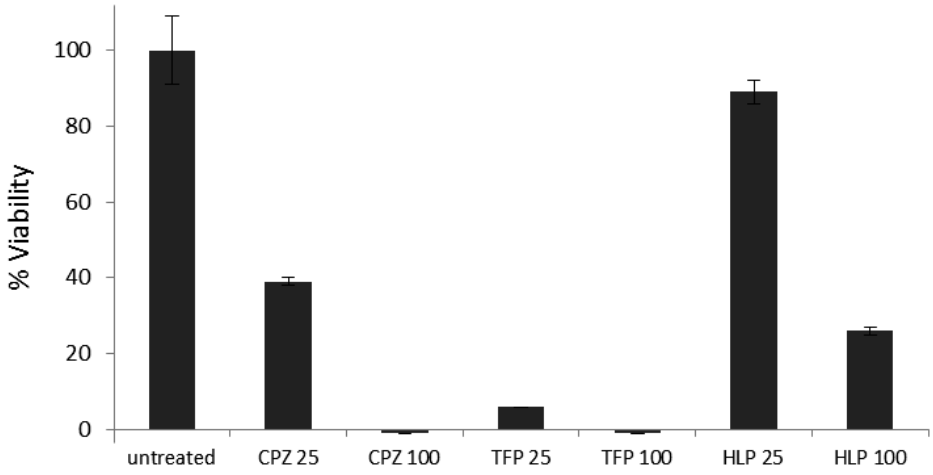

Figure 8. Effect of selected antipsychotic drugs (in pure form) on viability of U266 cells at 25 µM and 100 µM (24 h). CPZ, TFP, and HLP refer to chlorpromazine, trifluoperazine, and haloperidol, respectively. Each column represents the Mean±SD of technical replicates (n=5).

3.2 Dose and Time Dependent Inhibitory and Cytotoxic Effect of Trifluoperazine

In accordance with the potency screening results, the subsequent studies have been carried on with TFP since it has shown the most effective growth inhibition on U266 cells. Half maximal inhibitory concentration (IC_{50}) of TFP was determined as 15.4 ± 0.7 μM by treating cells with 12 different dose values ranging from 0.5 to 100 μM for 24 h (Figure 9).

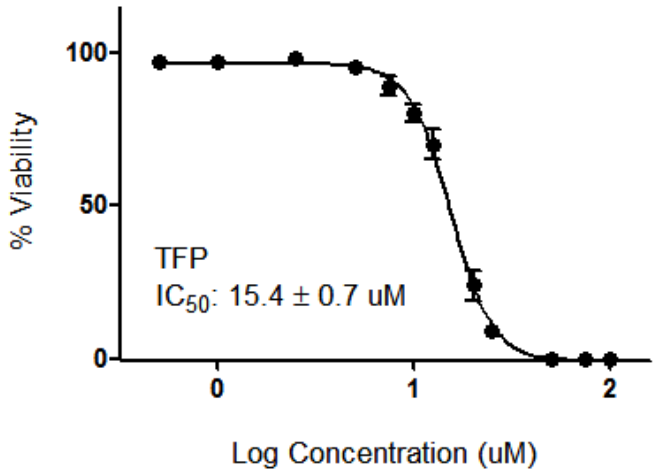

Figure 9. Dose response and potency (IC50) determination of TFP on the basis of its growth inhibitory effect on U266 cells. TFP concentration ranges from 0.5 to 100 μM. Data represents the Mean±SEM (n=2).

For all experiments in this thesis, cisplatin - an anticancer drug currently used also for multiple myeloma treatment -has been used as a positive control with its IC_{50} dose for U266 cell line (40 μM) [23].

Figure 10 shows the time dependent effect of 10 μM TFP on viability of U266 cells at three different time points. For 12, 24 and 48 h, cell viability was 86, 75 and 43%, respectively. There was a highly significant decrease on viability of cells especially from 24 h to 48 h treatment with $p<0.001$.

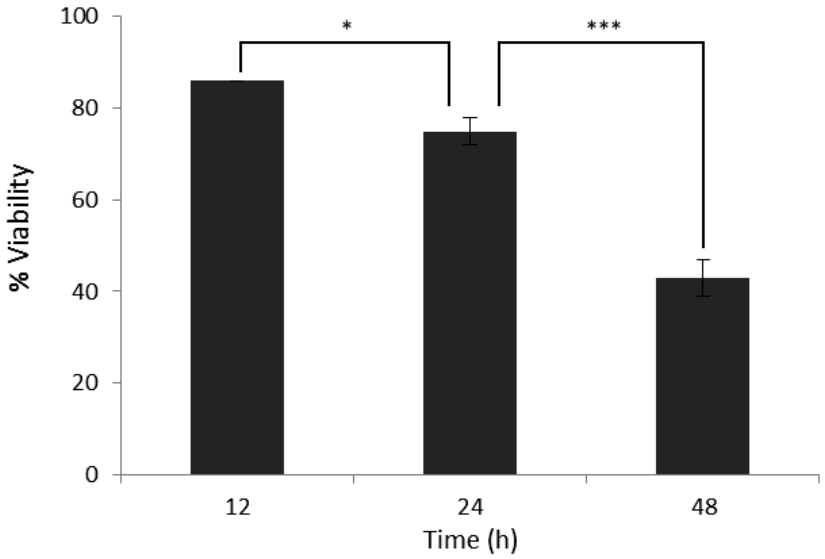

Figure 10. Time dependent effect of TFP on viability of U266 cells at 10 μM (12, 24 and 48 h). Results for each time point are normalized according to their untreated controls at the same time point. Each column represents the Mean±SEM (n=3). Asterisks * and *** denote statistical significance between 12 and 24h at $p<0.05$, 24 and 48h at $p<0.001$, respectively.

Even if these results demonstrate the cell growth inhibitory effect of TFP, which is both dose and time dependent, they do not answer whether this inhibition is based on cytotoxic or antiproliferative effect of TFP. Hence, to answer this question, MultiTox-Fluor Multiplex Cytotoxicity Assay was also performed. This assay measures cell viability and cytotoxicity simultaneously by using two different protease markers (GF-AFC for viability, bis-AAF-R110 for cytotoxicity), which differ in excitation and emission values [55]. According to results of this assay as shown in Figure 11, there is a high increase in cytotoxicty in addition to decrease in viability, which means that TFP has a significant cytotoxic effect on U266 cells at 15 μM for 24 h treatment with $p<0.01$.

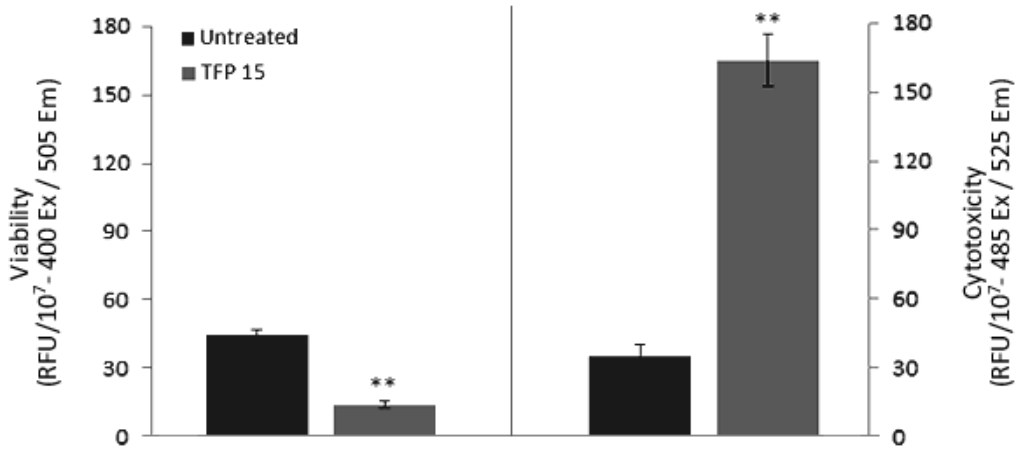

Figure 11. Cytotoxic effect of TFP on U266 cells at 15 μM (24 h) determined by MultiTox-Fluor assay, which measures viability and cytotoxicity simultaneously by using two different protease markers. Each column represents the Mean±SEM (n=2). Asterisks ** denote statistical significance at $p<0.01$.

3.3 Cell Cycle Analysis of U266 Cells Treated with Trifluoperazine

Although MultiTox-Fluor assay shows cytotoxic effect of TFP on U266 cell line, it does not give information about its antiproliferative effect. To investigate the effect of TFP on cell proliferation of U266 cells, cell cycle assay was conducted by staining cells with propidium iodide (PI) after treating with 15 μM TFP for 24 h and analyzed by flow cytometry. PI binds to double-stranded DNA and provides to measure DNA content of cells at a single time point by exhibiting fluorescence. This measurement is used to calculate the percentage of cells in G0/G1, S and G2/M phases [56].

The histogram in Figure 12-A shows the border of cell populations in G0/G1, S and G2/M phases. When looking the normalized values of each phase in Figure 12-B, although there was an increase at G2/M phase for treated cells, this increase was not significant. Changes in G0/G1 and S phases were also not significant. Cell

population of untreated and 15 μM TFP were 56±3 vs. 53±2 % in G0/G1, 15±1 vs. 11±2 % in S, 29±4 vs. 37±3 % in G2/M, respectively (n=3, p>0.05).

From these results, we concluded that TFP did not induce cell cycle arrest in U266 cell line.

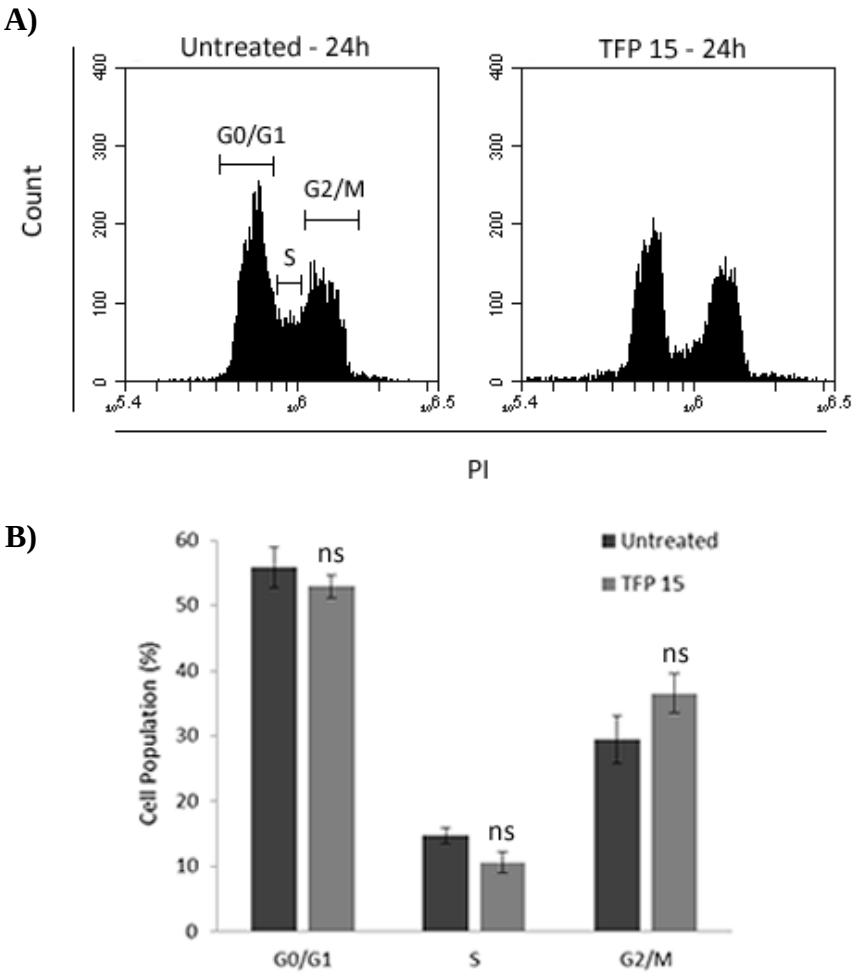

Figure 12. Effect of TFP on cell cycle of U266 cells at 15 μM (24 h) measured by flow cytometry. A) Representative fluorescence intensity histograms of cells stained with PI, where range of cell-cycle phases (G0/G1, S and G2/M) are shown on the upper-left panel. B) Bar plots of normalized cell population of each phase for untreated and TFP-treated cells, which are represented as Mean±SEM. There is no significant difference between treated and untreated cells for any of cell phases, where p>0.05 (n=3).

3.4 Apoptosis Studies of U266 Cells Treated with Trifluoperazine

Results showed that the cell growth inhibitory effect of TFP was due to its cytotoxic activity, but not cytostatic activity. Hence, another question needed to be answered. What was the underlying cell death mechanism of this cytotoxic activity? Was it related to apoptosis or not? To understand it, three common apoptosis assays were performed.

3.4.1 Effect of Trifluoperazine on Mitochondrial Membrane Potential (Δψ)

Change in mitochondrial membrane potential (Δψ) is one of the early events of apoptosis, which result in depolarization of mitochondria. JC-1, a membrane permeable lipophilic cationic fluorochrome, is used to determine the depolarization state of mitochondria. In healthy cells, mitochondria is polarized and JC-1 is uptaken into mitochondria rapidly and forms aggregates, which exhibits red fluorescence signal. In apoptotic cells, JC-1 cannot accumulate into mitochondria since mitochondrial membrane is depolarized, and remains in monomer form, which exhibits green fluorescence signal. Hence, it results in a decrease of red fluorescence signal when cells shifting from polarized to depolarized Δψ state [57].

In this study, U266 cells were stained with JC-1 to investigate the effect of TFP treatment (15 μM, 24 h) on Δψ and analyzed with flow cytometry (Figure 13). When depolarized percentages of treated cells are compared with untreated cells (10 and 9%, respectively) that were obtained from gated depolarization states in Figure 13-A according to shift in red fluorescence signal, there was no significant difference between two groups (n=3, $p>0.05$).

After these results, same experiment was performed for 12 h and 48 h at the same treatment dose (15 μM) to see whether these results were time dependent or not. JC-1 12 h and 48 h results also showed that there was no significant increase in

depolarized state of mitochondria when cells treated with TFP (Figure 16 - App. A). All these results mean that TFP-treated cells were JC-1 negative.

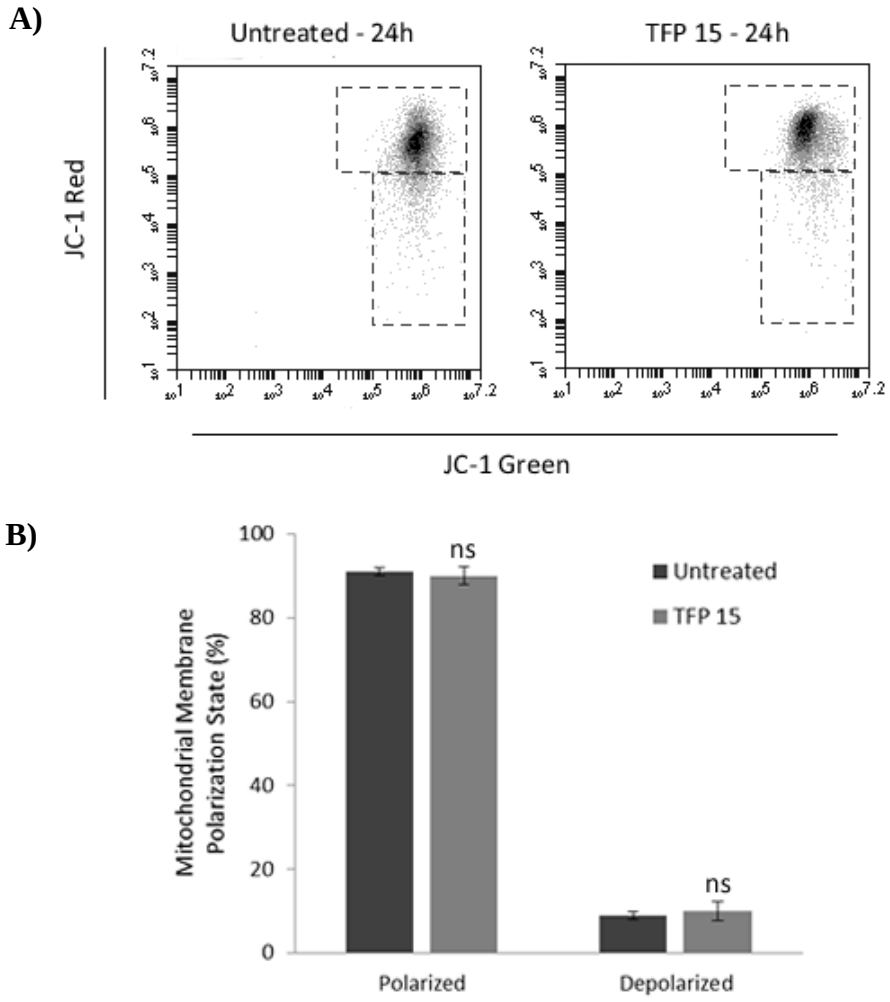

Figure 13. Effect of TFP on mitochondrial membrane potential (Δψ) of U266 cells at 15 μM (24 h) measured by flow cytometry. A) Representative fluorescence intensity dot plots of cells stained with JC-1, where gated polarized and depolarized states are shown. B) Bar plots of normalized Δψ state values for untreated and TFP-treated cells, which are represented as Mean±SEM. ns means that there is no significant difference between treated and untreated cells for both polarized and depolarized percentages, where $p>0.05$ (n=3).

3.4.2 Effect of Trifluoperazine on Caspase-3 Activity

Caspase-3 is one of the most important members of caspase family of cysteine proteases that plays a significant role in apoptosis. Like other caspase family members, it is found in an inactive pro-enzyme form in healthy cells. In cells undergoing apoptosis, it becomes active by self-cleavage and/or cleavage by other proteases. Hence, active caspase-3 is used as a marker for cells undergoing apoptosis [58].

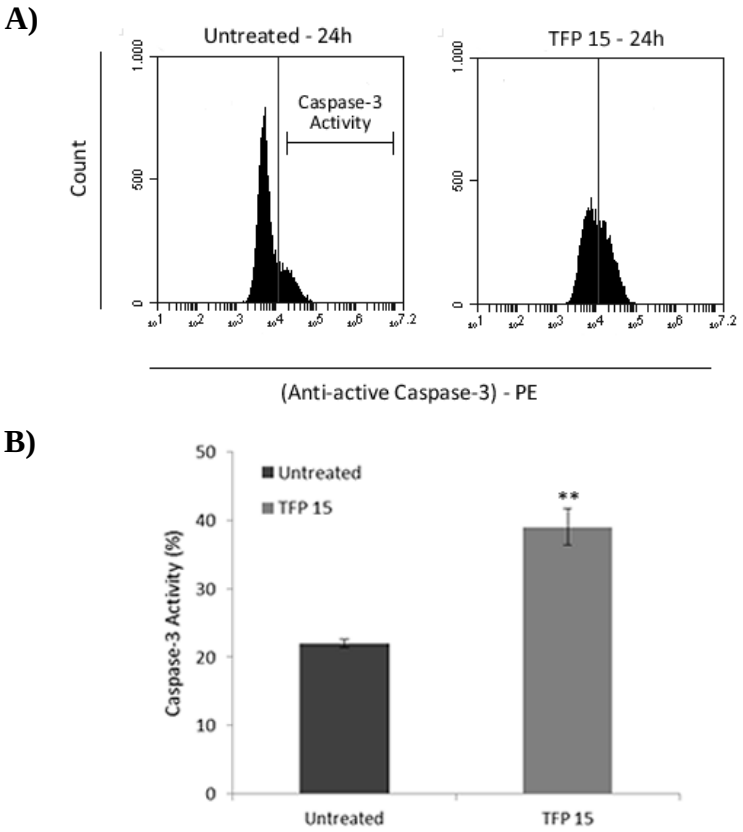

Figure 14. Effect of TFP on Caspase-3 activity of U266 cells at 15 μM (24 h) measured by flow cytometry. A) Representative fluorescence intensity histograms of cells stained with anti-active caspase-3 PE, where the intensity threshold for caspase-3 activity is shown on the upper-left panel. B) Bar plots of corresponding histograms for untreated and TFP-treated cells, which are represented as Mean±SEM. Asterisks ** denote statistical significance at $p<0.01$ (n=3).

According to the results in Figure 14, there was a significant effect of 15 μM TFP on Caspase-3 activity of U266 cells (22% untreated vs. 39% TFP) for 24 h treatment analyzed by flow cytometry (n=3, $p<0.01$). In other words, TFP-treated cells induced apoptosis through Caspase-3 activity.

3.4.3 Effect of Trifluoperazine on Cell Membrane Asymmetry

Another critical event occurring during apoptosis is loss of plasma membrane asymmetry as a result of translocation of phospholipid phosphatidylserine (PS) from the inner to the outer part of the membrane, which occurs in the earlier stages of apoptosis. Annexin-V (conjugated to PE) binds to externalized PS with a high affinity and used as an early apoptosis marker. Annexin-V is generally used together with 7-AAD, which is a late apoptosis marker since it can only penetrate into membranes of damaged or dead cells [59]. As seen in Figure 15-A, cells on the bottom-left quadrant of the panel (both AnnexinV-PE and 7-AAD negative) are viable, on the bottom-right ones (AnnexinV-PE positive, 7-AAD negative) are early apoptotic (EA), and on the upper-right ones (both AnnexinV-PE and 7-AAD positive) are late apoptotic (LA).

As the last analysis related with apoptosis in this study, the effect of 15 μM TFP (for 24 and 48 h treatment) on cell membrane asymmetry of U266 cells stained with Annexin V-PE and 7-AAD was measured by flow cytometry.

For both 24 and 48 h treatment results, there was a highly significant increase in treated cell population percent for EA and LA state while live cell population % was decreasing (Figure 15-B). For 24 h, cell population of untreated and 15 μM TFP were 67 vs. 32 % for live, 28 vs. 52 % for EA, 4 vs. 16 % for LA, respectively. For 48 h, cell population of untreated and 15 μM TFP were 69 vs. 8 % for live, 25 vs. 72 % for EA, 5 vs. 19 % for LA, respectively.

As a conclusion, cells treated with 15 μM TFP induced apoptosis as indicated in Annexin-V / 7-AAD assay.

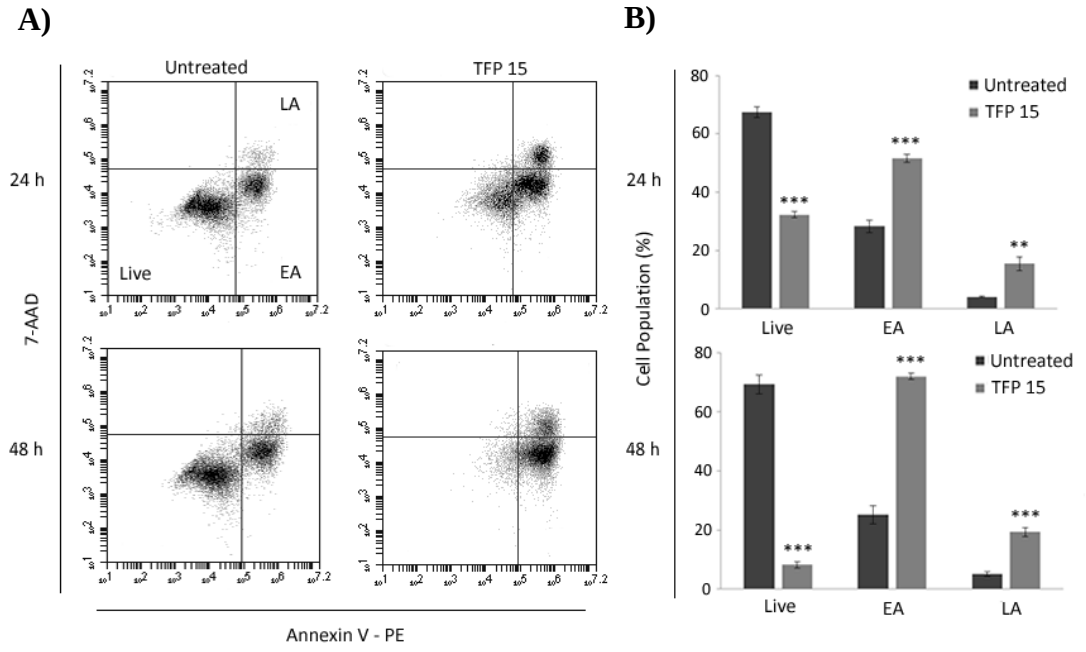

Figure 15. Effect of TFP on cell membrane asymmetry of U266 cells at 15 μM (24 and 48 h) measured by flow cytometry. A) Representative fluorescence intensity dot plots of cells stained with Annexin V-PE and 7-AAD, where the quadrants representing living, early apoptotic (EA) and late apoptotic (LA) cell population are shown on the upper-left panel. B) Bar plots of corresponding quadrants for untreated and TFP-treated cells, which are represented as Mean±SEM. Asterisks ** and *** denote statistical significance at $p<0.01$ and $p< 0.001$, respectively (n=3).

3.5 Combinatory Effect of Trifluoperazine and Cisplatin

In chemotherapy, combination of anticancer drugs is one of the most commonly used therapeutic approaches to break the resistance of cancer cells and to increase the efficiency of treatment [14].

Both trifluoperazine (TFP) and cisplatin (Cis) are highly effective in low μM ranges on U266 cell line, IC_{50} of which is around 15 μM and 40 μM, respectively. Based on their strong inhibitory effect on U266 cells, a combination study of TFP and Cis was conducted with four combined doses listed in Table 3. The treatment concentrations were chosen around IC_{50} values of these compounds. For each combined dose, Combination Index (CI) value was calculated using CompuSyn software according to growth inhibitory percentages of cells treated with these doses for 24 h, which were determined by CellTiter Blue assay. Combined doses with CI values > 1.10 show antagonism, CI values between 0.90 - 1.10 show additivity, and CI values < 0.90 show synergism (Table 5 - App. B).

From the results in Table 3, 10 μM TFP - 20 μM Cis and 10 μM TFP - 40 μM Cis combinations showed slightly antagonistic effect whereas 15 μM TFP - 20 μM Cis and 15 μM TFP - 40 μM Cis showed additive effect. Results were represented as the Mean±SEM (n=3).

Table 3. Combinatory effect of trifluoperazine and cisplatin

TFP (μM)	Cis (μM)	Combination Cytotoxicity (%)	Combination Index (CI)
15	40	67 ± 7	1.04 ± 0.04
15	20	59 ± 7	1.02 ± 0.03
10	40	54 ± 6	1.16 ± 0.07
10	20	42 ± 5	1.11 ± 0.04

According to these results, when Cis concentration increased and TFP concentration decreased, CI value increased. Hence, doses for the second set of experiment were determined based on this clue. Cis doses were decreased and TFP doses were increased to observe synergism by getting lower CI values. Cis concentrations were fixed as 15 μM for this time since changes in TFP doses affected CI values much more than changes in Cis doses.

Although CI values decreased when TFP concentration increased, results were similar with the first dataset (Table 4 - App. A), which was additive for 20 μM TFP - 15 μM Cis, and moderate antagonistic for 15 μM TFP - 15 μM Cis and 10 μM TFP - 15 μM Cis. As the last set of experiment, Cis concentrations were decreased a bit more. However, results were still either additive or slightly antagonistic (Table 4 - App. A).

CHAPTER 4

DISCUSSION

Drug repurposing has become a very popular strategy to find new therapies for diseases, especially for cancer, since it considerably reduces the cost and time necessary to develop a novel drug [60]. In this study, we revealed that trifluoperazine (TFP), an FDA-approved antipsychotic drug mainly used in the treatment of schizophrenia, has a dose and time dependent growth inhibitory and cytotoxic effect on p53-deficient multiple myeloma (MM) cell line U266. It did not show antiproliferative effect, but it induced apoptosis. There are various *in vitro* and *in vivo* studies showing anticancer effects of phenothiazine class of antipsychotics, particularly TFP, in cell lines of different cancer types such as leukemia, lymphoma, breast, lung, melanoma, prostate, and pancreatic cancer [35–41]. However, this is the first in-depth cytotoxicity and apoptosis study of TFP on MM.

We found the half maximal inhibitory concentration (IC_{50}) of TFP as 15.4 μM, which is in low micromolar (μM) range making it highly potent. Moreover, time response studies revealed that even 10 μM TFP treatment caused a significant decrease in cell viability (57%) after 48 h treatment. Dose response studies of TFP in the literature also give similar potency results. Hait W. N. et al. (1985) has determined IC_{50} of TFP as 5 μM on L1210 leukemic lymphocytes (72 h treatment) [35]. In another study (Krstic M., 2011), it has been determined as 20.2, 18.5, 17.5, and 20.5 μM on MCF-7 (breast cancer cell line), MDA-MB-453 (breast cancer cell line), SW-480 (colon cancer cell line), and IM9 (multiple myeloma cell line), respectively, for 48 h treatment [61].

We also showed that the cell growth inhibitory effect of TFP was due to its cytotoxic activity on U266 cells. In many studies, cytotoxic effect of TFP is linked to its calmodulin blocking activity since calmodulin is essential for cells due to its role in cellular processes, signaling pathways, cell proliferation, regulation of cell motility and division [40,62,63]. Furthermore, there are studies showing that TFP is not toxic to normal cells despite its cytotoxic effects on cancer cells [64]. This selective cytotoxicity of TFP may be explained by the fact that calmodulin levels are generally higher in malignant cells than normal cells [65]. However, the main problem with TFP is its achievable plasma concentration. In a clinical study, it was calculated as 320 μM, which was almost 50 times lower than IC_{50} concentration of TFP on U266 cells calculated in this study [66]. This problem may be achieved by using controlled drug delivery systems such as injection of drug encapsulated with liposome [67].

We also investigated the antiproliferative effect of TFP by cell cycle analysis. Results showed that there was a slight increase in G2/M phase, yet it was not statistically significant. It means that TFP did not show arrest on cell cycle, therefore it was not able to prevent proliferation of U266 cells. However, there are studies demonstrating the induction of cell cycle arrest at G1/S or G2/M boundaries by calmodulin antagonists, which are associated with the essential role of calmodulin in cell proliferation [68,69]. The reason of having different results from the literature may be explained by p53 mutant characteristic of U266 cell line, which is a tumor suppressor gene triggering cell cycle arrest or apoptosis depending on physiological conditions. The p53 gene product is an important cell cycle check-point regulator at both the G1/S and G2/M check points [70].

We conducted three apoptosis assays to investigate the cell death mechanism underlying the cytotoxic effect of TFP on U266 cells. According to our results, while TFP increased Caspase-3 activity and caused to loss of membrane integrity, it did not cause depolarization of mitochondrial membrane.

It is actually not surprising that TFP did not lead to mitochondrial membrane depolarization since it is also a mitochondrial permeability transition (MPT) pore inhibitor. MPT has a critical role in apoptotic cell death. When MPT is promoted via various factors such as Ca^{2+}, reactive oxygen species (ROS), inorganic phosphate etc., MPT pores open and substances begin to move into mitochondrial membrane non-selectively, which leads to depolarization of mitochondria [71]. Hence, blocking this activity keeps the mitochondria to stay in polarized state. There are a few studies which also support this argument [72–74]. Moreover, there are studies showing Fas-mediated apoptosis of TFP-treated cells, which is one of the death receptor pathways [62,63]. Therefore, apoptotic effect of TFP on cancer cells may result from triggering extrinsic pathway (death receptor pathway) instead of intrinsic pathway (mitochondrial pathway). No matter which pathway is triggered, both of them converge on the same event, caspase-3 activation. Once it is activated, a series of irreversible events take action leading to the death of the cell, which include loss of membrane asymmetry, DNA fragmentation, degradation of nuclear proteins, and formation of apoptotic bodies that finally uptaken by phagocytes [75].

Lastly, based on the strong inhibitory effect of TFP and cisplatin on U266 cells, we conducted a combination study with various doses of two compounds. Cisplatin is a platinum compound commonly used in chemotherapy. It interacts with DNA and activates specific signaling pathways by forming DNA crosslink adducts. As a result, it induces apoptosis [76]. In this combination study, results were additive for higher doses of TFP, and slightly antagonistic for lower doses of TFP. In another combination study of TFP and cisplatin in the literature, results were highly dependent on the type of cell line. While TFP-cisplatin combination showed antagonistic effect on OVCAR-4 cell line, it showed additivity on OVCAR-3, and synergism on 2780-C8 [77]. There are many combination studies of TFP with other chemotherapeutic drugs such as doxorubicin and bleomycin [46,48]. It is generally used as an efflux blocker and enhances the cytotoxic activity of chemotherapeutic agents by blocking the function of PGP and sensitizing MDR cells to chemotherapeutic agents [48]. However, in this study, we showed that TFP induces

apoptosis on MM cells. Hence, it is also a candidate as a cytotoxic agent for MM treatment apart from its MDRi function. One of the best strategies in combination therapy is to combine a cytotoxic drug with a cytostatic agent [14]. Based on this strategy, combination of TFP with a cytostatic agent such as flavopiridol, which is a CDK inhibitor and arrests cell cycle at the G1/S and G2/M transition, may be evaluated. Moreover, combination potential of TFP with bortezomib and lenalidomide, which are commonly used for MM treatment, can be investigated in future studies.

CHAPTER 5

CONCLUSION

In this study, dose and time-dependent growth inhibitory and cytotoxic effect of TFP was shown on U266 MM cell line. Its IC_{50} value was in low micromolar (μM) range, which makes it highly potent. The cytotoxic effect of TFP was probably related with its calmodulin blocking activity. Moreover, it was not toxic to normal cells according to the literature. Although it did not show antiproliferative effect, it induced apoptosis on p53-deficient cell line U266. TFP-cisplatin combination was additive with higher doses of TFP, and slightly antagonistic with lower doses of TFP. Its combinational potential with cytostatic agents such as flavopiridol or with agents used in MM treatment including bortezomib and lenalidomide may also be evaluated in future studies.

In addition to being a calmodulin antagonist, TFP is also a chemosensitizer due to its MDR inhibition function. Moreover, it is an FDA-approved drug, and cheap. When considering all these factors and our findings, TFP becomes a powerful candidate to be repurposed for MM treatment, and it warrants further in-depth mechanistic studies and *in vivo* experiments.

REFERENCES

[1] L. Naymagon and M. AbdulHay, "Novel agents in the treatment of multiple myeloma: a review about the future," *J. Hematol. Oncol.*, 2016.

[2] J. R. Berenson, *Biology and Management of Multiple Myeloma*, vol. 53, no. 9. 2004.

[3] "Myeloma - SEER Stat Fact Sheets." [Online]. Available: http://seer.cancer.gov/statfacts/html/mulmy.html. [Accessed: 10-Aug-2016].

[4] R. A. Kyle and S. V. Rajkumar, "ASH 50th anniversary review," *Blood*, vol. 111, no. 6, pp. 2962–2972, 2008.

[5] "What is multiple myeloma?" [Online]. Available: https://www.themmrf.org/multiple-myeloma/what-is-multiple-myeloma/. [Accessed: 05-Aug-2016].

[6] M. T. Drayson, "Using single protein biomarkers to predict health and disease in diverse patient populations: a new role for assessment of immunoglobulin free light chains.," *Mayo Clin. Proc.*, vol. 87, no. 6, pp. 505–7, 2012.

[7] S. Iida, "Mechanisms of action and resistance for multiple myeloma novel drug treatments.," *Int. J. Hematol.*, pp. 0–1, 2016.

[8] S. C. Gupta, B. Sung, S. Prasad, L. J. Webb, and B. B. Aggarwal, "Cancer drug discovery by repurposing: Teaching new tricks to old dogs," *Trends Pharmacol. Sci.*, vol. 34, no. 9, pp. 508–517, 2013.

[9] I. M. Ghobrial, P. G. Richardson, and K. C. Anderson, *Bortezomib in the Treatment of Multiple Myeloma*. 2008.

[10] R. N. Ganapathi and M. K. Ganapathi, "Mechanisms regulating resistance to inhibitors of topoisomerase II," *Front. Pharmacol.*, vol. 4 AUG, no. August, pp. 1–7, 2013.

[11] A. Persidis, "Cancer multidrug resistance.," *Nat. Biotechnol.*, vol. 17, pp. 94–95, 1999.

[12] R. C. Fernando, F. De Carvalho, D. R. Mazzotti, F. Evangelista, W. Moisés, T. Braga, and M. D. L. Chauffaille, "Multiple myeloma cell lines and primary tumors proteoma : protein biosynthesis and immune system as potential therapeutic targets," vol. 6, no. November, 2015.

[13] J. F. San Miguel, "Introduction to a series of reviews on multiple myeloma," *Blood*, vol. 125, no. 20, pp. 3039–3040, 2015.

[14] D.-Y. Lu, *Personalized Cancer Chemotherapy*, vol. 1542, no. 9. 2015.

[15] M. A. Shah and G. K. Schwartz, "Cell Cycle-mediated Drug Resistance: An Emerging Concept in Cancer Therapy ," *Clin. Cancer Res.* , vol. 7 , no. 8 , pp. 2168–2181, 2001.

[16] "U266B1 [U266] ATCC ® TIB-196™ Homo sapiens peripheral blood." [Online]. Available: https://www.lgcstandards-atcc.org/Products/All/TIB-196.aspx#generalinformation. [Accessed: 02-Aug-2016].

[17] M. Rowley, P. Liu, and B. Van Ness, "Heterogeneity in therapeutic response of genetically altered myeloma cell lines to interleukin 6, dexamethasone, doxorubicin, and melphalan.," *Blood*, vol. 96, no. 9, pp. 3175–80, 2000.

[18] R. Catlett-Falcone, T. H. Landowski, M. M. Oshiro, J. Turkson, A. Levitzki, R. Savino, G. Ciliberto, L. Moscinski, J. L. Fernández-Luna, G. Nuñez, W. S. Dalton, and R. Jove, "Constitutive activation of Stat3 signaling confers resistance to apoptosis in human U266 myeloma cells.," *Immunity*, vol. 10, no. 1, pp. 105–15, 1999.

[19] C. C. Harris, "Structure and function of the p53 tumor suppressor gene: clues for rational cancer therapeutic strategies.," *J. Natl. Cancer Inst.*, vol. 88, no. 20, pp. 1442–1455, 1996.

[20] C. A. Brady and L. D. Attardi, "P53 At a Glance," *J. Cell Sci.*, vol. 123, no. 15, pp. 2527–2532, 2010.

[21] J. T. Zilfou and S. W. Lowe, "Tumor suppressive functions of p53.," *Cold Spring Harb. Perspect. Biol.*, vol. 1, no. 5, pp. 1–12, 2009.

[22] C. J. Brown, S. Lain, C. S. Verma, A. R. Fersht, and D. P. Lane, "Awakening guardian angels: drugging the p53 pathway.," *Nat. Rev. Cancer*, vol. 9, no. 12, pp. 862–873, 2009.

[23] İ. Z. Durusu, "Anticancer effect and combination potential of clofazimine in

multiple myeloma," *MS Thesis METU*, 2016.

[24] A. Biber, "Nortriptyline, a tricyclic antidepressant, induces apoptosis in U266 multiple myeloma cell line," *MS Thesis METU*, 2016.

[25] D. M. Gardner, R. J. Baldessarini, and P. Waraich, "Modern antipsychotic drugs: A critical overview," *Cmaj*, vol. 172, no. 13, pp. 1703–1711, 2005.

[26] H. Buschmann, J. L. Díaz, J. Holenz, A. Párraga, A. Torrens, and J. M. Vela, *Antidepressants, Antipsychotics, Anxiolytics*, vol. 1. 2007.

[27] M. Dold, M. T. Samara, C. Li, M. Tardy, and S. Leucht, "Haloperidol versus first-generation antipsychotics for the treatment of schizophrenia and other psychotic disorders.," *Cochrane database Syst. Rev.*, vol. 1, no. 1, p. CD009831, 2015.

[28] "Dopamine - Stress & Anxiety Reduction." [Online]. Available: http://anxietyrelieftraining.com/dopamine/. [Accessed: 05-Aug-2016].

[29] J. Kuhlmann and W. Puls, "Handbook of Experimental Pharmacology Volume 119-Oral Antidiabetics," vol. 120, pp. 421–426, 1996.

[30] A. Jaszczyszyn, K. Gąsiorowski, P. Świątek, W. Malinka, K. Cieślik-Boczula, J. Petrus, and B. Czarnik-Matusewicz, "Chemical structure of phenothiazines and their biological activity," *Pharmacol. Reports*, vol. 64, no. 1, pp. 16–23, 2012.

[31] L. Qi and Y. Ding, "Potential antitumor mechanisms of phenothiazine drugs," *Sci. China Life Sci.*, vol. 56, no. 11, pp. 1020–1027, 2013.

[32] "trifluoperazine | C21H24F3N3S - PubChem." [Online]. Available: https://pubchem.ncbi.nlm.nih.gov/compound/trifluoperazine#section=Top. [Accessed: 05-Aug-2016].

[33] K. Yuan, S. Yong, F. Xu, T. Zhou, J. M. McDonald, and Y. Chen, "Calmodulin antagonists promote TRA-8 therapy of resistant pancreatic cancer.," *Oncotarget*, vol. 6, no. 28, pp. 25308–25319, 2015.

[34] "trifluoperazine | C21H24F3N3S - PubChem." [Online]. Available: https://pubchem.ncbi.nlm.nih.gov/compound/trifluoperazine#section=DrugBank-Interactions&fullscreen=true. [Accessed: 05-Aug-2016].

[35] W. N. Hait, L. Grais, C. Benz, and E. C. Cadman, "Inhibition of growth of

leukemic cells by inhibitors of calmodulin : Phenothiazines and melittin," pp. 202–205, 1985.

[36] S. Naftalovichl, E. Yefenof, and Y. Eilaml, "Antitumor effects of ketoconazole and trifluoperazine in murine T-cell lymphomas," *Cancer Chemother. Pharmacol.*, pp. 384–390, 1991.

[37] S.-H. Park, Y. M. Chung, J. Ma, Q. Yang, J. S. Berek, M. C.-T. Hu, S.-H. Park, Y. M. Chung, J. Ma, Q. Yang, J. S. Berek, and M. C.-T. Hu, "Pharmacological activation of FOXO3 suppresses triple-negative breast cancer in vitro and in vivo," *Oncotarget*, vol. 5, no. 0, 2016.

[38] Q. Chen, L. J. Wu, Y. Q. Wu, G. H. Lu, Z. Y. Jiang, J. W. Zhan, Y. Jie, and J. Y. Zhou, "Molecular mechanism of trifluoperazine induces apoptosis in human A549 lung adenocarcinoma cell lines," *Mol. Med. Rep.*, vol. 1, no. 5, pp. 811–817, 2009.

[39] I. Gil-Ad, B. Shtaif, Y. Levkovitz, J. Nordenberg, M. Taler, I. Korov, and A. Weizman, "Phenothiazines induce apoptosis in a B16 mouse melanoma cell line and attenuate in vivo melanoma tumor growth," *Oncol. Rep.*, vol. 15, no. 1, pp. 107–112, 2006.

[40] A. Sivanandam, S. Murthy, K. Chinnakannu, R. Barrack, M. Menon, and G. P. Reddy, "Calmodulin protects androgen receptor from calpain-mediated breakdown in prostate cancer cells," *J Cell Physiol.*, vol. 226, no. 7, pp. 1889–1896, 2012.

[41] K. Yuan, G. Jing, J. Chen, H. Liu, K. Zhang, Y. Li, H. Wu, J. M. McDonald, and Y. Chen, "Calmodulin mediates Fas-induced FADD-independent survival signaling in pancreatic cancer cells via activation of Src-Extracellular Signal-regulated Kinase (ERK)," *J. Biol. Chem.*, vol. 286, no. 28, pp. 24776–24784, 2011.

[42] T. Tsuruo, H. Iida, S. Tsukagoshi, and Y. Sakurai, "Increased accumulation of vincristine and Adriamycin in drug-resistant P388 tumor cells following incubation with calcium antagonists and calmodulin inhibitors," *Cancer Res.*, vol. 42, no. 11, pp. 4730–4733, 1982.

[43] J. Wei, R. A. Hickie, and D. J. Klaassen, "Inhibition of Human Breast Cancer Colony Formation," pp. 86–90, 1983.

[44] P. J. Smith, J. Mircheva, and N. M. Bleehen, "Interaction of bleomycin, hyperthermia and a calmodulin inhibitor (trifluoperazine) in mouse tumor cells," *Int. J. Radiat. Oncol. Biol. Phys.*, vol. 12, no. 8, pp. 1363–1366, 1986.

[45] R. Ganapathi, H. Schmidt, D. Grabowski, M. Melia, and N. Ratliff, "Modulation in vitro and in vivo of cytotoxicity but not cellular levels of doxorubicin by the calmodulin inhibitor trifluoperazine is dependent on the level of resistance.," *Br. J. Cancer*, vol. 58, no. 3, pp. 335–340, 1988.

[46] W. N. Hait, S. Morris, J. S. Lazo, R. J. Figlin, H. J. Durivage, K. White, and P. E. Schwartz, "Phase I trial of combined therapy with bleomycin and the calmodulin antagonist, trifluoperazine," *Cancer Chemother. Pharmacol.*, vol. 23, no. 6, pp. 358–362, 1989.

[47] G. T. Budd, R. M. Bukowski, A. Lichtin, L. Bauer, P. Van Kirk, and R. Ganapathi, "Phase II trial of doxorubicin and trifluoperazine in metastatic breast cancer," *Invest. New Drugs*, vol. 11, no. 1, pp. 75–79, 1993.

[48] M. Lehnert, R. De Giuli, K. Kunke, S. Emerson, W. S. Dalton, and S. E. Salmon, "Serum can inhibit reversal of multidrug resistance by chemosensitisers," *Eur. J. Cancer*, vol. 32, no. 5, pp. 862–867, 1996.

[49] C. Ramachandran, W. You, and A. Krishan, "Bcl-2 and mdr-1 gene expression during doxorubicin-induced apoptosis in murine leukemic P388 and P388/R84 cells.," *Anticancer Res.*, vol. 17, no. 5A, pp. 3369–76, 1997.

[50] G. Pan, S. Vickers, A. Pickens, and J. Phillips, "Apoptosis and Tumorigenesis in Human," *Am. J. Pathol.*, vol. 155, no. 1, 1999.

[51] S. Y. Shin, C. G. Kim, D. D. Hong, and J. Kim, "Implication of Egr-1 in trifluoperazine-induced growth inhibition in hum an U87M G gliom a cells," vol. 36, no. 4, pp. 380–386, 2004.

[52] C. T. Yeh, A. T. H. Wu, P. M. H. Chang, K. Y. Chen, C. N. Yang, S. C. Yang, C. C. Ho, C. C. Chen, Y. L. Kuo, P. Y. Lee, Y. W. Liu, C. C. Yen, M. Hsiao, P. J. Lu, J. M. Lai, L. S. Wang, C. H. Wu, J. F. Chiou, P. C. Yang, and C. Y. F. Huang, "Trifluoperazine, an antipsychotic agent, inhibits cancer stem cell growth and overcomes drug resistance of lung cancer," *Am. J. Respir. Crit. Care Med.*, vol. 186, no. 11, pp. 1180–1188, 2012.

[53] A. Pulkoski-Gross, J. Li, C. Zheng, Y. Li, N. Ouyang, B. Rigas, S. Zucker, and J. Cao, "Repurposing the antipsychotic trifluoperazine as an antimetastasis agent.," *Mol. Pharmacol.*, vol. 87, no. 3, pp. 501–12, 2015.

[54] Promega, "CellTiter-Blue ® Cell Viability Assay," vol. TB317, pp. 3–16, 2016.

[55] B. A. L. Niles, R. a Moravec, M. Scurria, W. Daily, P. D, L. Bernad, B.

Mcnamara, P. Guthmiller, K. Rashka, D. Lange, M. Arduengo, T. L. Riss, and P. Corporation, “MultiTox-Fluor Multiplex Cytotoxicity Assay,” pp. 20–23, 2006.

[56] P. Pozarowski and Z. Darzynkiewicz, “Analysis of cell cycle by flow cytometry.,” *Methods Mol. Biol.*, vol. 281, pp. 301–311, 2004.

[57] BD Biosciences, “Flow Cytometry Mitochondrial Membrane Potential Detection Kit Instruction Manual,” no. 551302, pp. 1–20, 2013.

[58] BD Pharmingen, “Technical Data Sheet PE Active Caspase-3 Apoptosis Kit,” pp. 2–3.

[59] BD Pharmingen, “Technical Data Sheet PE Annexin V Apoptosis Detection Kit I,” vol. 3942, no. September 2005, pp. 3–11, 2013.

[60] B. McCabe, F. Liberante, and K. I. Mills, “Repurposing medicinal compounds for blood cancer treatment.,” *Ann. Hematol.*, vol. 94, no. 8, pp. 1267–76, 2015.

[61] M. Krstić, S. P. Sovilj, S. Grgurić-Šipka, I. R. Evans, S. Borozan, and J. F. Santibanez, “Synthesis, structural and spectroscopic characterization, in vitro cytotoxicity and in vivo activity as free radical scavengers of chlorido(p-cymene) complexes of ruthenium(II) containing N-alkylphenothiazines,” *Eur. J. Med. Chem.*, vol. 46, no. 9, pp. 4168–4177, 2011.

[62] Y. Chen, P. Pawar, G. Pan, L. Ma, H. Liu, and J. M. McDonald, “Calmodulin binding to the Fas-mediated death-inducing signaling complex in cholangiocarcinoma cells,” *J. Cell. Biochem.*, vol. 103, no. 3, pp. 788–799, 2008.

[63] X. Wu, E.-Y. Ahn, and M. A. McKenna, “Fas Binding to Calmodulin Regulates Apoptosis in Osteoclasts,” *J Biol Chem.*, vol. 4, no. 164, pp. 29964–29970, 2005.

[64] Z. Zhelev, H. Ohba, R. Bakalova, V. Hadjimitova, M. Ishikawa, Y. Shinohara, and Y. Baba, “Phenothiazines suppress proliferation and induce apoptosis in cultured leukemic cells without any influence on the viability of normal lymphocytes: Phenothiazines and leukemia,” *Cancer Chemother. Pharmacol.*, vol. 53, no. 3, pp. 267–275, 2004.

[65] F. Grief, H. S. Soroff, K. M. Albers, and L. B. Taichman, “The effect of trifluoperazine, a calmodulin antagonist, on the growth of normal and malignant epidermal keratinocytes in culture,” *Eur. J. Cancer Clin. Oncol.*,

vol. 25, no. 1, pp. 19–26, 1989.

[66] M. Raderer and W. Scheithauer, “Clinical trials of agents that reverse multidrug resistance: A literature review,” *Cancer*, vol. 72, no. 12, pp. 3553–3563, 1993.

[67] R. Krishna, M. S. Webb, G. St Onge, and L. D. Mayer, “Liposomal and nonliposomal drug pharmacokinetics after administration of liposome-encapsulated vincristine and their contribution to drug tissue distribution properties.,” *J. Pharmacol. Exp. Ther.*, vol. 298, no. 3, pp. 1206–1212, 2001.

[68] S. Gangopadhyay, P. Karmakar, U. Dasgupta, and A. Chakraborty, “Trifluoperazine stimulates ionizing radiation induced cell killing through inhibition of DNA repair.,” *Mutat. Res.*, vol. 633, no. 2, pp. 117–25, 2007.

[69] M. W. Berchtold and A. Villalobo, “The many faces of calmodulin in cell proliferation, programmed cell death, autophagy, and cancer,” *Biochim. Biophys. Acta - Mol. Cell Res.*, vol. 1843, no. 2, pp. 398–435, 2014.

[70] C. H. Golias, a. Charalabopoulos, and K. Charalabopoulos, “Cell proliferation and cell cycle control : a mini review,” *Int. J. Clin. Pract.*, vol. 58, no. 12, pp. 1134–1141, 2004.

[71] J. S. Kim, L. He, and J. J. Lemasters, “Mitochondrial permeability transition: A common pathway to necrosis and apoptosis,” *Biochem. Biophys. Res. Commun.*, vol. 304, no. 3, pp. 463–470, 2003.

[72] S. Muranaka, T. Kanno, H. Fujita, H. Kobuchi, J. Akiyama, T. Yasuda, and K. Utsumi, “Involvement of ceramide in the mechanism of Cr(VI)-induced apoptosis of CHO cells,” *Free Radic. Res.*, vol. 38, no. 6, pp. 613–621, 2004.

[73] V. Petronilli, C. Cola, and P. Bernardi, “Modulation of the Mitochondrial Cyclosporin A-sensitive Permeability,” *J. Biol. Chem.*, vol. 5, no. 2, pp. 1011–1016, 1993.

[74] F. D. Toledo, L. M. Pérez, C. L. Basiglio, J. E. Ochoa, E. J. Sanchez Pozzi, and M. G. Roma, “The Ca2+-calmodulin-Ca2+/calmodulin-dependent protein kinase II signaling pathway is involved in oxidative stress-induced mitochondrial permeability transition and apoptosis in isolated rat hepatocytes,” *Arch. Toxicol.*, vol. 88, no. 9, pp. 1695–1709, 2014.

[75] S. Elmore, “Apoptosis: A Review of Programmed Cell Death,” *Toxicol Pathol.*, vol. 35, no. 4, pp. 495–516, 2007.

[76] Z. H. Siddik, “Cisplatin: mode of cytotoxic action and molecular basis of resistance,” *Oncogene*, vol. 22, no. 47, pp. 7265–7279, Oct. 2003.

[77] R. P. Perez, L. M. Handel, and T. C. Hamilton, “Potentiation of cisplatin cytotoxicity in human ovarian carcinoma cell lines by trifluoperazine, a calmodulin inhibitor,” *Gynecol. Oncol.*, vol. 46, no. 1, pp. 82–87, 1992.

APPENDICES

APPENDIX A

SUPPLEMENTARY DATA

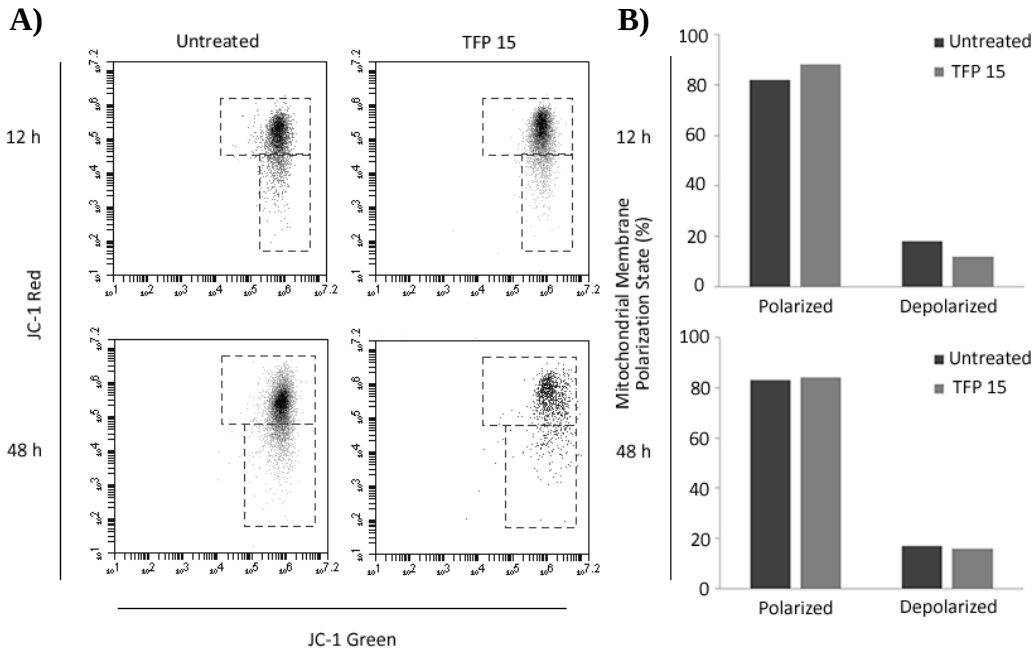

Figure 16. Effect of TFP on mitochondrial membrane potential (Δψ) of U266 cells at 15 μM (12 and 48 h) measured by flow cytometry.

Table 4. Combinatory effect of trifluoperazine and cisplatin

TFP (μM)	Cis (μM)	Combination Cytotoxicity (%)	Combination Index (CI)
20	15	79	1.00
15	15	56	1.27
10	15	39	1.32
25	10	86	1.01
20	10	68	1.09
15	10	46	1.11

APPENDIX B

COMBINATION INDEX (CI) TABLE

Table 5. Reccommended symbols and descriptions for combination index ranges

Combination Index (CI) Range	symbol	description
<0.1	+++++	very strong synergism
0.1-0.3	++++	strong synergism
0.3-0.7	+++	synergism
0.7-0.85	++	moderate synergism
0.85-0.90	+	slight synergism
0.90-1.10	+ -	nearly additive
1.10-1.20	-	slight antagonism
1.20-1.45	--	moderate antagonism
1.45-3.3	---	antagonism
3.3-10	----	strong antagonism
>10	-----	very strong antagonism